Report No. FAA-RD-78-135

POOL FIRE RADIATION THROUGH A DOOR IN A SIMULATED AIRCRAFT FUSELAGE

THOR I. EKLUND

DECEMBER 1978

FINAL REPORT

Prepared for

U.S. DEPARTMENT OF TRANSPORTATION
FEDERAL AVIATION ADMINISTRATION
Systems Research & Development Service
Washington, D.C. 20590

Technical Report Documentation

1. Report No.	2. Government Accession No.	3. Recipient's Catalog No.
FAA-RD-78-135		

4. Title and Subtitle	5. Report Date
POOL FIRE RADIATION THROUGH A DOOR IN A SIMULATED AIRCRAFT FUSELAGE	December 1978
	6. Performing Organization Code
7. Author(s)	8. Performing Organization Report No.
Thor I. Eklund	FAA-NA-78-38
9. Performing Organization Name and Address Federal Aviation Administration National Aviation Facilities Experimental Center Atlantic City, New Jersey 08405	10. Work Unit No. (TRAIS)
	11. Contract or Grant No. 181-521-000
12. Sponsoring Agency Name and Address U.S. Department of Transportation Federal Aviation Administration Systems Research and Development Service Washington, D.C. 20590	13. Type of Report and Period Covered Final August 1977-December 1977
	14. Sponsoring Agency Code ARD-520

15. Supplementary Notes

16. Abstract

This study evaluates small-scale methods of simulating postcrash fuel spill fires adjacent to fuselage open doors. Pool fires in a quiescent environment were scaled down and their radiant heat transfer through fuselage doorways evaluated. Steel ducts of 1-, 2-, 3-, and 4-foot diameter were employed as models. Analytic solutions to radiative transfer equations were developed and matched with the experimental heat fluxes at two locations within each model. The analysis demonstrates that the doorway can be treated as a radiating black body surface of 1,874 degrees Fahrenheit (^{o}F), and that heat fluxes to other areas around the doorway can be calculated. A comparison of heat flux to the model exterior was compared with existing full-scale fire test data.

17. Key Words	18. Distribution Statement
Radiation Scaling Fuel Fire Cabin Fire Aircraft	Document is available to the U.S. public through the National Technical Information Service, Springfield, Virginia 22161

19. Security Classif. (of this report)	20. Security Classif. (of this page)	21. No. of Pages	22. Price
Unclassified	Unclassified	41	

Form DOT F 1700.7 (8-72) Reproduction of completed page authorized

METRIC CONVERSION FACTORS

Approximate Conversions to Metric Measures

Symbol	When You Know	Multiply by	To Find	Symbol
		LENGTH		
in	inches	*2.5	centimeters	cm
ft	feet	30	centimeters	cm
yd	yards	0.9	meters	m
mi	miles	1.6	kilometers	km
		AREA		
in^2	square inches	6.5	square centimeters	cm^2
ft^2	square feet	0.09	square meters	m^2
yd^2	square yards	0.8	square meters	m^2
mi^2	square miles	2.6	square kilometers	km^2
	acres	0.4	hectares	ha
		MASS (weight)		
oz	ounces	28	grams	g
lb	pounds	0.45	kilograms	kg
	short tons (2000 lb)	0.9	tonnes	t
		VOLUME		
tsp	teaspoons	5	milliliters	ml
Tbsp	tablespoons	15	milliliters	ml
fl oz	fluid ounces	30	milliliters	ml
c	cups	0.24	liters	l
pt	pints	0.47	liters	l
qt	quarts	0.95	liters	l
gal	gallons	3.8	liters	l
ft^3	cubic feet	0.03	cubic meters	m^3
yd^3	cubic yards	0.76	cubic meters	m^3
		TEMPERATURE (exact)		
°F	Fahrenheit temperature	5/9 (after subtracting 32)	Celsius temperature	°C

*1 in = 2.54 (exactly). For other exact conversions and more detailed tables, see NBS Misc. Publ. 286, Units of Weights and Measures, Price $2.25, SD Catalog No. C13.10:286.

Approximate Conversions from Metric Measures

Symbol	When You Know	Multiply by	To Find	Symbol
		LENGTH		
mm	millimeters	0.04	inches	in
cm	centimeters	0.4	inches	in
m	meters	3.3	feet	ft
m	meters	1.1	yards	yd
km	kilometers	0.6	miles	mi
		AREA		
cm^2	square centimeters	0.16	square inches	in^2
m^2	square meters	1.2	square yards	yd^2
km^2	square kilometers	0.4	square miles	mi^2
ha	hectares (10,000 m^2)	2.5	acres	
		MASS (weight)		
g	grams	0.035	ounces	oz
kg	kilograms	2.2	pounds	lb
t	tonnes (1000 kg)	1.1	short tons	
		VOLUME		
ml	milliliters	0.03	fluid ounces	fl oz
l	liters	2.1	pints	pt
l	liters	1.06	quarts	qt
l	liters	0.26	gallons	gal
m^3	cubic meters	35	cubic feet	ft^3
m^3	cubic meters	1.3	cubic yards	yd^3
		TEMPERATURE (exact)		
°C	Celsius temperature	9/5 (then add 32)	Fahrenheit temperature	°F

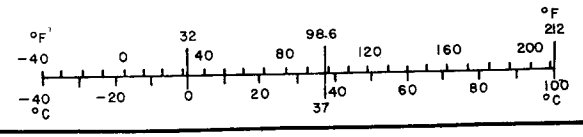

PREFACE

The assistance of Messrs. Louis J. Brown, William E. Neese, and Joseph A. Wright in the varying activities of instrumentation, testing, and data analysis is acknowledged.

TABLE OF CONTENTS

LIST OF ILLUSTRATIONS

LIST OF TABLES

INTRODUCTION

PURPOSE.

The purpose of this program is to evaluate small-scale cabin fire tests as a means for more economical but suitably realistic aircraft fire testing. The report describes the experimental results of heat transfer through the doors of simulated fuselages subjected to external pool fires in a quiescent atmosphere. A mathematical procedure is developed which allows calculation of radiant heat fluxes to the cabin interior on a point-by-point basis.

BACKGROUND.

In the event of a postcrash aircraft fire, survival of the passengers may depend on the environment of the cabin interior during the time interval required for evacuation. Because of the large quantities of aviation kerosene carried aboard commercial jets and its potential for release and ignition during a crash, the effect of external fuel fires on the fuselage and its interior must be defined if cabin safety improvements are to be realistically evaluated. Past full-scale tests on a narrow body fuselage subjected to pool fires (reference 1) showed that aluminum panels on the aircraft skin melted within 40 seconds. The thicker aluminum skins and insulation of wide-body jets may yield additional time before the fuselage fails to provide protection to cabin occupants.

Prior to thermal failure of the fuselage, an external fuel fire threatens the cabin interior through its effect on any openings--fuselage breaks, opened doors, or melted windows. Any fire penetration or radiative flux provides a potential for fire involvement with interior materials before the fuselage itself would fail through melting. Because of the potential of these interior materials to yield heat, smoke, and toxic gases, such material involvement might jeopardize the passengers prior to thermal failure of the fuselage.

Full-scale tests of the effect of pool fires on the fuselage have examined the heat flux to the aircraft skin under varying wind conditions (references 1, 2, 3). Although the data varies considerably with fire placement and wind conditions, these tests provide a realistic spectrum of heat transfer values that can be expected in postcrash fire. Heat transfer values as high as 13 British thermal units per foot squared second (Btu/ft^2 s) were documented in one set of tests (reference 1), 16 Btu/ft^2 s in another (reference 2), and 18 Btu/ft^2 s in tests on a titanium fuselage (reference 3). These are upper extremes; the measured fluxes are typically between 1 and 8 Btu/ft^2 s. The average flux from reference 3 was 12 Btu/ft^2 s. Wind conditions are the dominant cause of this variability.

The characterization of a free standing pool fire has been the subject of exhaustive investigation (references 4, 5, 6, 7, 8, 9, 10). This is due to the hazard associated with pool fires in the oil industry as well as from spills from transport vehicles. Extensive data exist on heat fluxes from

these pool fires (references 8, 9, 10), and a number of predictive techniques for the heat flux have been developed (references 11, 12). A number of conclusions from these studies have a bearing on small-scale aircraft fire tests. First, the pool fire becomes fully turbulent at about 3-feet in diameter. Also, the flame becomes optically thick at a pool diameter between 3 and 10 feet. For test purposes, a 3-foot fire can be considered optically thick. The existing data indicate that the pool fires can be scaled down to 3 feet but still maintain the radiative characteristics of large fires. This scalability of the pool fire suggests that radiative exposure of material and structures to large fires could be adequately tested with relatively small pool fires. Furthermore, for radiative exposure, a 1-foot diameter fuselage adjacent to a 4-foot fire, shown in figure 1, is considered equivalent to a 20-foot fuselage adjacent to an 80-foot fire. Varying the fire size could be simulated by changing the fuselage size and maintaining a constant fire size.

This type reasoning can be applied to measure radiative flux through a fuselage opening in a quiescent atmosphere. In a wind environment, additional scaling factors may be required since the tilt angle of a flame in a constant wind is a function of fire size (reference 13).

The development of a methodology for scaling the interaction of a fuselage with a pool fire has several applications. First, small-scale testing provides a means for economically developing a broad data base to support full-scale tests. Second, small-scale testing offers a promising method for evaluating cabin interior materials as to their ignitability when subjected to a highly realistic radiative source. Pool fires show time-dependent fluctuations in their radiative output even when their time-averaged flux is repeatable. This type fluctuation is not easily reproduced by radiant heaters in laboratory-type material flammability tests.

EXPERIMENTAL OBJECTIVE.

The experimental objective of these quiescent pool fire tests was: (1) to quantify the radiative heat transfer from a pool fire through a fuselage opening, (2) to determine the repeatability of the test, and (3) to develop the methodology for conducting such tests. The testing involved different combinations of fuselage diameter, pool fire size, and distance between fuselage and fire.

DISCUSSION

TEST CONFIGURATION.

Figure 2 shows an overall view of the test configuration. The tests were performed in a warehouse-type building which is 102-foot long and 39-foot wide. The side walls are 20-foot high, and the roof has a 26-foot peak running the length of the building. The fires were set under the peak and 20 feet from the front of the building. Each test article was a 10-foot long

open-ended duct simulating a fuselage. Each duct interior was insulated with Kaowool®, a noncombustible ceramic fibrous insulation, to prevent any reradiation from the wall to the sensors inside. All radiative flux would, therefore, enter through a simulated cabin door. The door was sized to geometrical scale with the door of the C-133 fuselage used concurrently for full-scale fire tests (reference 14). Figure 3 shows the end view of the duct and pan configuration and the dimensions of the four ducts used, along with significant measurements of fire placement and sensor location. The fuel pans were all placed in a larger water pan to prevent warping of the fuel pan during the fire. Kaowool insulation was placed between the duct and pans to prevent air from flowing upwards at this juncture. The fire was ignited by an electric spark and extinguished by two remotely actuated nozzles connected to a Cardox® system.

The primary sensors were calorimeters within the doorway and radiometers set around the fire pan. The data were recorded on a Honeywell model 1858 cathode ray tube (CRT) Visicorder. Figures 4, 5, 6, and 7 show the placement of the calorimeters and radiometers in the doorway. The calorimeters are Hy-Cal model C-1300A, and the radiometers are Hy-Cal model R-8015C with calcium fluoride windows. Figure 4 shows the interior of the 4-foot duct with the radiometer riding piggyback on the calorimeter. They are both supported on a traversing mechanism which allows horizontal and vertical motion along the midplane of the ducts. Also visible is a calorimeter mounted in an upward-facing configuration midway between the traversing calorimeter and the door edge. This calorimeter senses the heat flux that flooring materials might undergo from an external fire at the doorway. Figures 5, 6, and 7 show the same calorimeters and radiometers as placed in the doorways of the 3-, 2-, and 1-foot diameter ducts, respectively. In these cases, the heat sensors are rigidly held, and the horizontally facing sensors are located at the duct midplane.

TEST DEVELOPMENT.

Numerous preliminary tests were performed with the 4-foot diameter duct. Figure 8 shows a data trace of radiometer output from an early test. For ease of data reduction, the fluctuations were electrically damped by addition of a 50-microfarad capacitor to each calorimeter and radiometer amplifier. A damped oscillograph trace is shown and labeled in figure 9. The tests were generally limited to a 60-second duration to prevent overheating of the building roof structure. The 20-second buildup time on the calorimeters was typical. A steady-state heat flux would remain until the end of the test when the action of the carbon dioxide (CO_2) extinguishers would momentarily increase the heat transfer to the calorimeters.

With the 4-foot duct, the 3-foot-square fuel pan was not representative of door exposure to a large fuel fire. The fire flattened itself against the duct with some loss in radiative thickness. In addition, random bending of the fire would uncover the door. The consistency of the data was significantly improved by use of a 4-foot-square fuel pan, and test repeatability was markedly improved and heat flux values increased as the fuselage was reduced in diameter. This indicates that the sideways bending of the flame is still a problem with the 4-foot duct. With smaller ducts, the duct door faced low

TABLE 1. INTERIOR HEAT FLUX WITH FIRE ADJACENT TO FUSELAGE

Date/Run	Duct Diameter (ft)	Midplane Cal (C_1) (Btu/ft^{2}s)	Floor Cal (C_2) (Btu/ft^{2}s)	C_2/C_1
12/22/6	1	1.8	2.4	1.3
7	1	1.8	2.6	1.4
8	1	1.7	2.5	1.5
12/15/1	2	1.7	2.3	1.4
2	2	1.8	2.4	1.3
3	2	1.7	2.4	1.4
12/16/1	2	1.8	2.4	1.3
2	2	1.8	2.4	1.3
3	2	1.9	2.5	1.3
12/21/1	2	1.7	2.2	1.3
2	2	1.8	2.4	1.3
12/29/1	2	1.8	2.7	1.5
2	2	1.9	2.6	1.4
3	2	1.9	2.6	1.4
12/23/12	3	1.7	2.2	1.3
13	3	1.8	2.3	1.3
14	3	1.7	2.3	1.3
10/28/4	4	1.7	2.3	1.4
11/9/5	4	2.1	2.1	1.0
6	4	1.4	0.9	0.6
11/17/1	4	1.5	1.9	1.3
2	4	1.4	1.8	1.3
11/29/1*	4	1.5	-	-
2*	4	1.2	-	-
3*	4	1.4	-	-
4*	4	1.3	-	-
11/30/1*	4	1.7	-	-
2*	4	1.8	-	-

* In these tests, the fuselage door faced a fire pan 5.5 feet long (distance perpendicular to fuselage) and 4.5 feet wide. In the rest of the tests the fire pan was 4 feet by 4 feet.

- No data collected.

enough into the fire to be unaffected by the flame bending. Figures 10, 11, 12, and 13 show examples of the fire geometry from the 4-, 3-, 2-, and 1-foot diameter ducts, respectively. Tests were also conducted with the fires offset from the fuselage as shown in figure 14.

Trial and error tests were performed to find the fuel quantity required for consistent fire radiative energy. Fuel quantities were incrementally increased until no additional radiative output was noted. In the 4-foot pan fires, 4 gallons of JP-4 were found to be an adequate fuel quantity. In a given sequence of tests, fuel was replenished after each 1-minute fire so that a minimum of 4 gallons was present at the start of each test. Although some distillation did occur during a test and although different fuel cuts could result in somewhat different radiative output (reference 4), this effect was not considered a serious problem for these tests.

Placement of the pool fire directly under the building peak was essential because any offset from the building center resulted in bending of the fire towards the building peak.

No fire penetration through the door into the duct was noted in these tests. Because the ducts were open ended, air could presumably feed the fire by passing through the duct out of the door and into the fire. A typical view of the fire from inside the duct is shown in figure 15a. Figure 15b shows a flame pulse over the doorway. This phenomenon was evidenced as a periodic pulsing of fire at the upper end of the door.

Since fire radiation through doorways was not studied during prior full-scale testing nearly so extensively as fuselage burn-through, some limited measurements of heat flux to the skin of the 2-foot duct were made. The two calimeters are shown in figure 16.

TEST DATA.

The primary information from these tests is the calorimeter data at the fuselage midplane and on the cabin floor. This data show the heat fluxes that cabin interior materials might experience from pool fire radiation through an open doorway. Table 1 provides the data points from tests with ducts of 1-, 2-, 3-, and 4-foot diameters adjacent to a 4-foot pool fire. From the data it is clear that the test repeatability is better with the smaller ducts as the heat flux approaches a value of 1.8 Btu/ft^2 s at the fuselage midplane and 2.5 Btu/ft^2 s on the floor. The variability in the data for the 4-foot duct in part arises from the bending of the fire enough to uncover the door. The differences in fluxes may also be partly due to the fact that the doors on the smaller ducts look into relatively lower portions of the fire.

Table 2 shows calorimeter data for 4-foot-square pool fires separated from the fuselage. Included in this table is data for different sized ducts. In table 1 when the 4-foot diameter duct was employed, the peak calorimeter readings were taken approximately 40 seconds into the test. The traversing mechanism was started 20 seconds into the test and reached the middle of the door at approximately 40 seconds into the test. In data for 1-, 2-, and 3-foot

diameter ducts, reported in table 1, the peak sensor value between 25 and 35 seconds after ignition was used. In cases of pans adjacent to ducts, this was generally a satisfactory procedure. However, in tests with the fuel pan offset from the duct, the recorded fluxes on the calorimeters continued to rise slightly through the 25- to 35-second period. The peak flux generally occurred between 40 and 45 seconds into the test and could rise as much as 30 percent higher than the values shown in table 2. However, values were taken within the 25- to 35-second interval for comparison with results shown in table 1. Although the sensed heat flux of both interior calorimeters dropped as the fire is moved away from the duct, the calorimeter on the floor showed the most dramatic reduction. The reason for this is that while the midplane calorimeter still senses fire over most of the doorway, the floor calorimeter "sees" vertically through the opening to regions where no fire is visible.

TABLE 2. INTERIOR HEAT FLUX WITH FIRE SEPARATED FROM FUSELAGE

Date/ Run	Duct Diameter (ft)	Distance Between Duct and Fire Pan (ft)	Midplane Calorimeter (Btu/ft^2s)	Floor Calorimeter (Btu/ft^2s)
12/22/9	1	2	1.3	.7
10	1	2	1.2	.5
11	1	2	1.3	.8
12/21/3	2	2	1.1	.7
4	2	2	1.2	.8
5	2	2	1.1	.7
12/23/15	3	2	.8	.3
16	3	2	1.0	.4
17	3	2	.9	.3
10/28/1	4	4	.5	.3
2	4	4	.5	.2
3	4	2	.8	.6

The appendix shows the development of the equations for predicting the heat flux to the internal calorimeters from an external pool fire. This development involves the solution of the view factor integral equations and the selection of appropriate fire temperatures and emissivities. The ratio of the heat flux to the floor calorimeter to the flux to the midplane calorimeter is simply the ratio of their shape factors to the fuselage door. This number is calculated to be 1.35 and agrees remarkably well with the ratios shown in table 1. Assuming an emissivity of 1, the appendix shows an average fire temperature of 1,874 degrees Fahrenheit (^oF) will produce a heat flux of 1.8 Btu/ft^2 s at the midplane calorimeter. This temperature is consistent

RESULTS

The experimental results of tests with fuselage models subjected to pool fire radiation through doorways can be summarized in four quantitative statements.

1. The heat flux to the midplane of the fuselage is 1.8 Btu/ft^2 s.

2. The heat flux to the floor one quarter of the way across the fuselage is 2.5 Btu/ft^2 s.

3. The heat flux to the skin of the fuselage around the doorway is between 12 and 14 Btu/ft^2 s on a 2-foot duct exposed to a 4-foot-square fire.

4. An analytical method for calculation of radiant heat through an open door to the cabin interior from an external fuel fire was developed and matched to the experimental data.

CONCLUSIONS

1. Small-scale test procedures for measuring a radiative flux through openings of simulated fuselages are feasible and lead to several additional conclusions.

2. A 4-foot pan fire provides a highly repeatable radiation source for 1-, 2-, and 3-foot diameter fuselages.

3. Scaled tests of pool fire effects on fuselages in a quiescent atmosphere require control of fuel depth and pan size to achieve repeatable tests. Fire plume instability, as evidenced in bending, results in a less controllable source of data variability.

4. As the pool fire is displaced from the fuselage, the midplane radiation in the cabin becomes larger than radiation to the floor calorimeter; the opposite is true when the pool fire is adjacent to the fuselage opening.

5. The heat flux to surfaces around the doorway within the fuselage can be calculated if the door surface is considered to be a black body radiator at a temperature of 1,874° F.

6. The method developed for calculating heat flux on the cabin interior from an external pool fire should be further validated by full-scale tests.

REFERENCES

1. Geyer, G.B., Effect of Ground Crash Fire on Aircraft Fuselage Integrity, Federal Aviation Administration, Report No. FAA-RD-69-46, 1969.

2. Conley, D.W., Post-Crash Fire-Fighting Studies on Transport Category Aircraft, Federal Aviation Administration, Report No. FAA-RD-65-50, 1965.

3. Sarkos, C.P., Titanium Fuselage Environmental Conditions in Post-Crash Fires, Federal Aviation Administration, Report No. FAA-RD-71-3, 1971.

4. Fu, T.T., Aviation Fuel Fire Behavior Study, Department of Defense, Aircraft Fire Suppression and Rescue Systems Office, Report No. AGFSRS-72-2, 1972.

5. Fu, T.T., Heat Radiation From Fires of Aviation Fuels, Fire Technology, 10, 54, 1974.

6. Hägglund, B., The Heat Radiation from Petroleum Fires, FoU-brand, 1, 18, 1977.

7. Gordon, W. and McMillan, R.D., Temperature Distribution Within Aircraft-Fuel Fires, Fire Technology, 1, 52, 1965.

8. Graves, K.W., Fire Fighter's Exposure Study, Department of Defense, Aircraft Fire Suppression and Rescue Systems Office, Report No. AGFSRS-71-2, 1970.

9. Alger, R.S. and Capener, E.L., Aircraft Ground Fire Suppression and Rescue Systems, Tri-Service System Program Office for Aircraft Ground Fire Suppression and Rescue, Report No. AGFSRS-72-1, 1972.

10. Capener, E.L. and Alger, R.S., Characterization and Suppression of Aircraft Fuel Fires, Western States Fall Meeting of the Combustion Institute, Paper WSCI-72-26, 1972.

11. Modak, A.T., Thermal Radiation from Pool Fires, Combustion and Flame, 29, 177, 1977.

12. Atallah, S. and Allan, D.S., Safe Separation Distances from Liquid Fuel Fires, Fire Technology, 7, 47, 1971.

13. Pipkin, O.A. and Sliepcevich, C.M., Effect of Wind on Buoyant Diffusion Flames, I&EC Fundamentals, 3, 147, 1964.

14. Sarkos, C.P. and Hill, R.G., Preliminary Wide Body (C133) Cabin Hazard Measurements During a Postcrash Fuel Fire, Federal Aviation Administration, National Aviation Facilities Experimental Center, Report NA-78-28-LR, 1978.

15. Sparrow, E.M. and Cess, R.D., Radiation Heat Transfer, Brooks/Cole Publishing Company, Belmont, California, 1970.

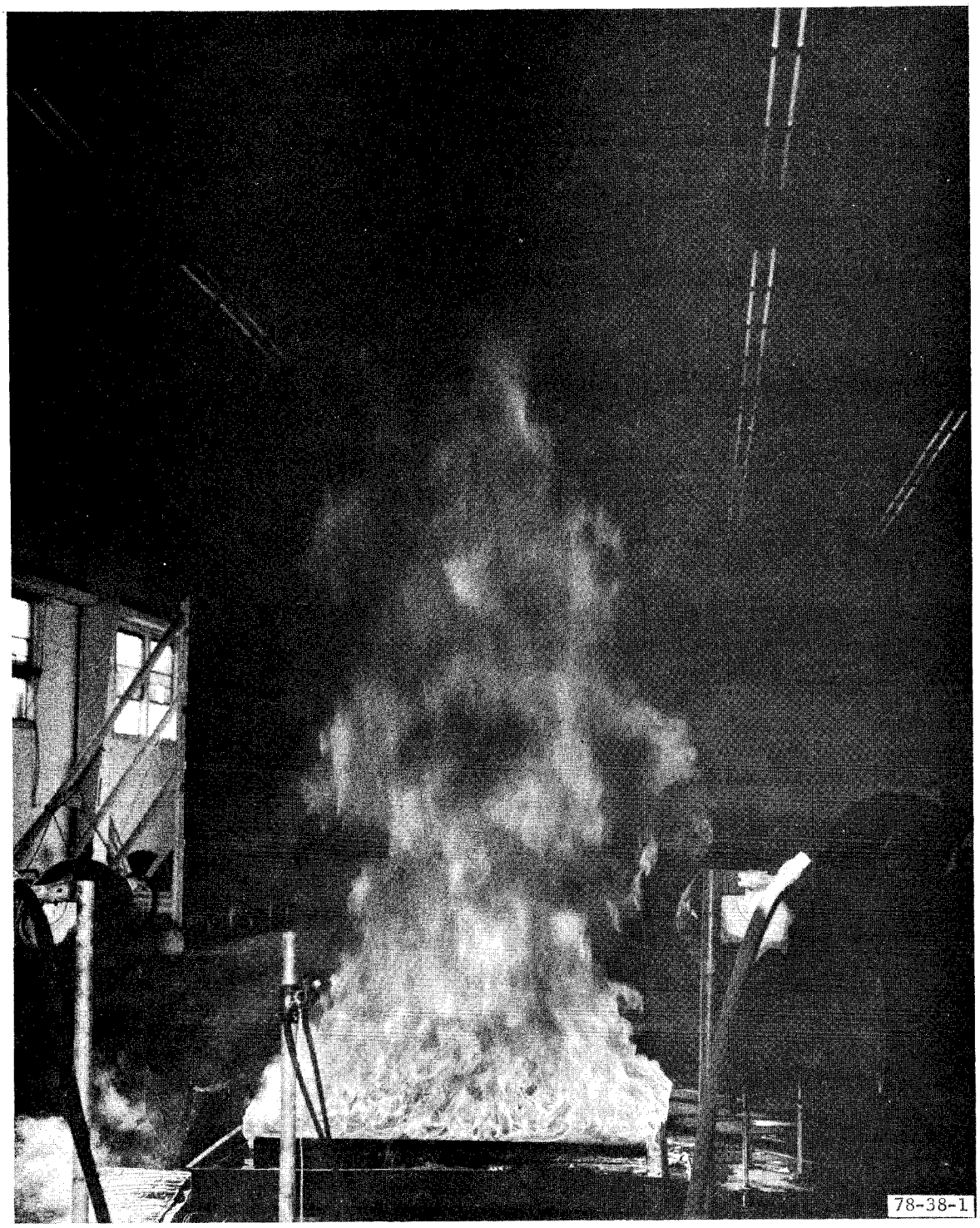

FIGURE 1. FOUR-FOOT PAN FIRE

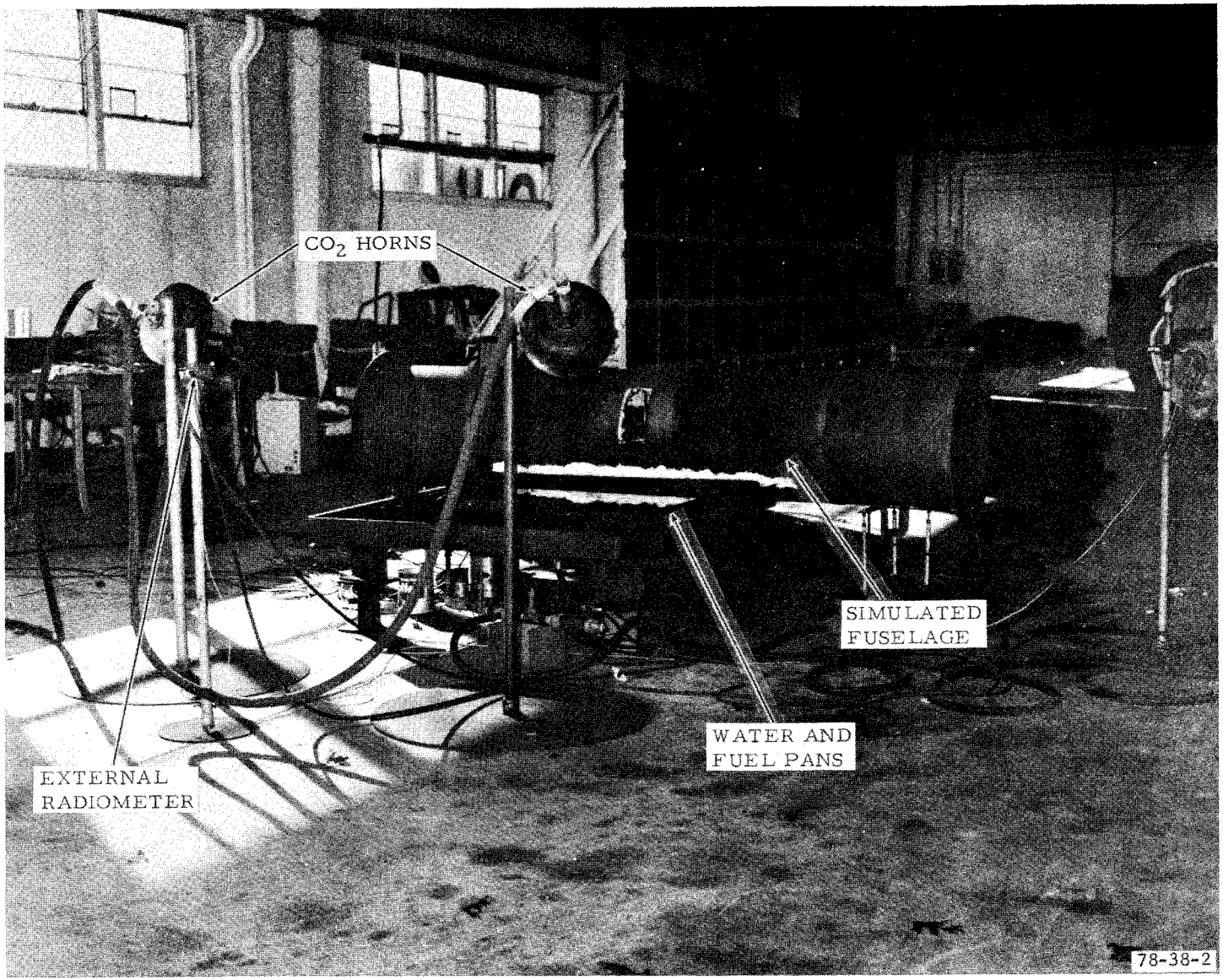

FIGURE 2. OVERALL TEST CONFIGURATION

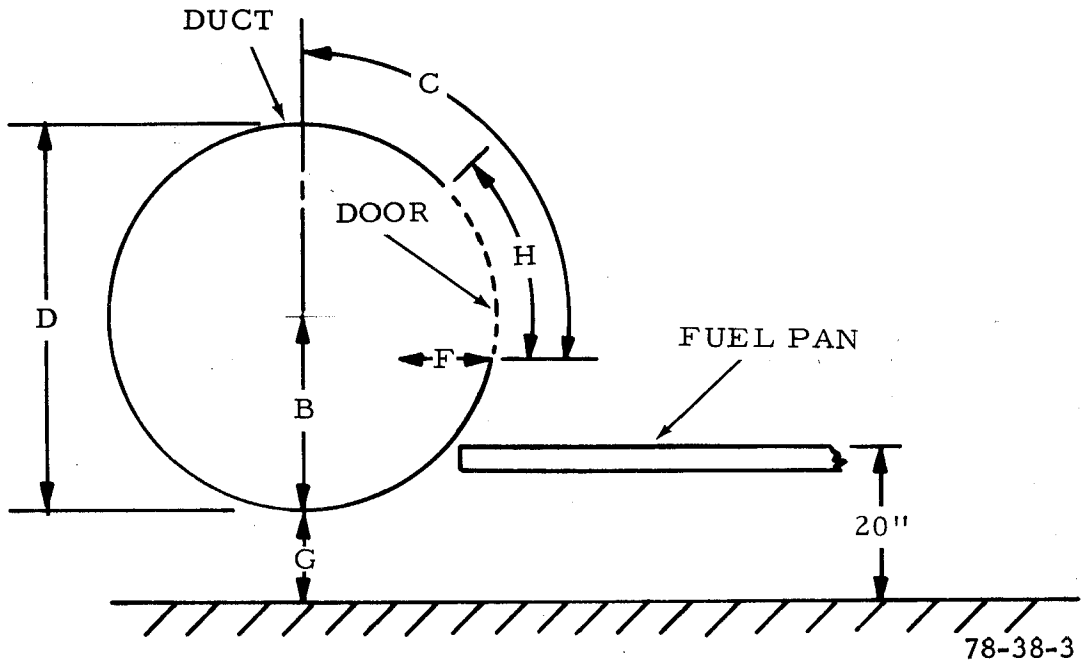

(D) Duct Diameter (ft)	(G) Height Of Duct Bottom Above Ground (in)	(C) Circumferential Distance From Duct Top To Door Bottom (in)	(H) Circumferential Door Height (in)	(W) Door Width (in)	(B) Height Of Midplane Calorimeter Above Duct Bottom (in)	(F) Distance Between Floor Calorimeter And Door (in)
4	10	41	20 5/8	10	29	12
3	12 1/2	27	16	8	22	9
2	15	20 1/2	10 3/4	5 1/8	14 1/2	6
1	17 1/2	10	5 3/8	2 5/8	7	3

NOTE: Distance Between Top Of Fuel Pan and Ground 20 Inches

FIGURE 3. END VIEW OF DUCT AND PAN CONFIGURATION

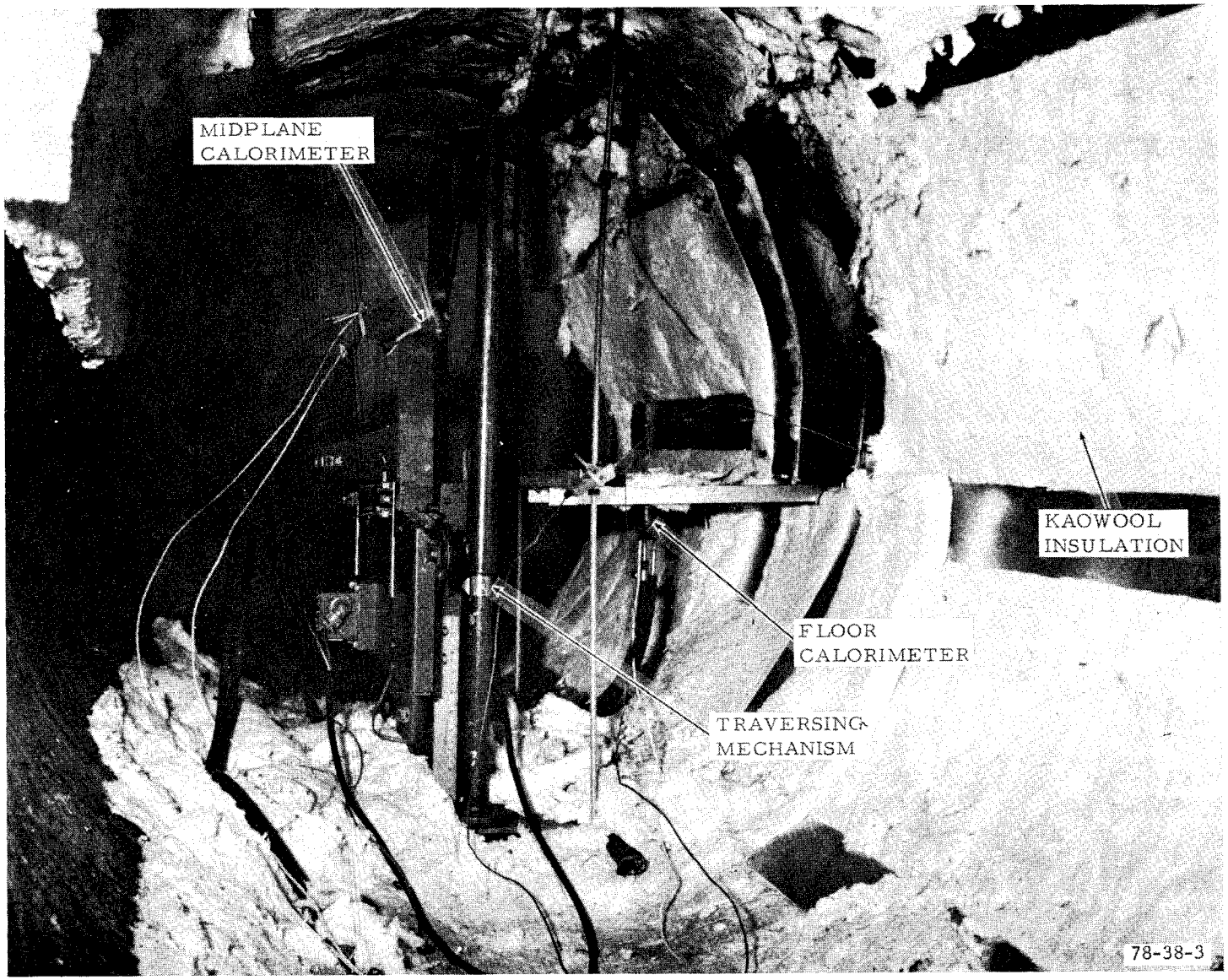

FIGURE 4. SENSORS IN 4-FOOT DUCT

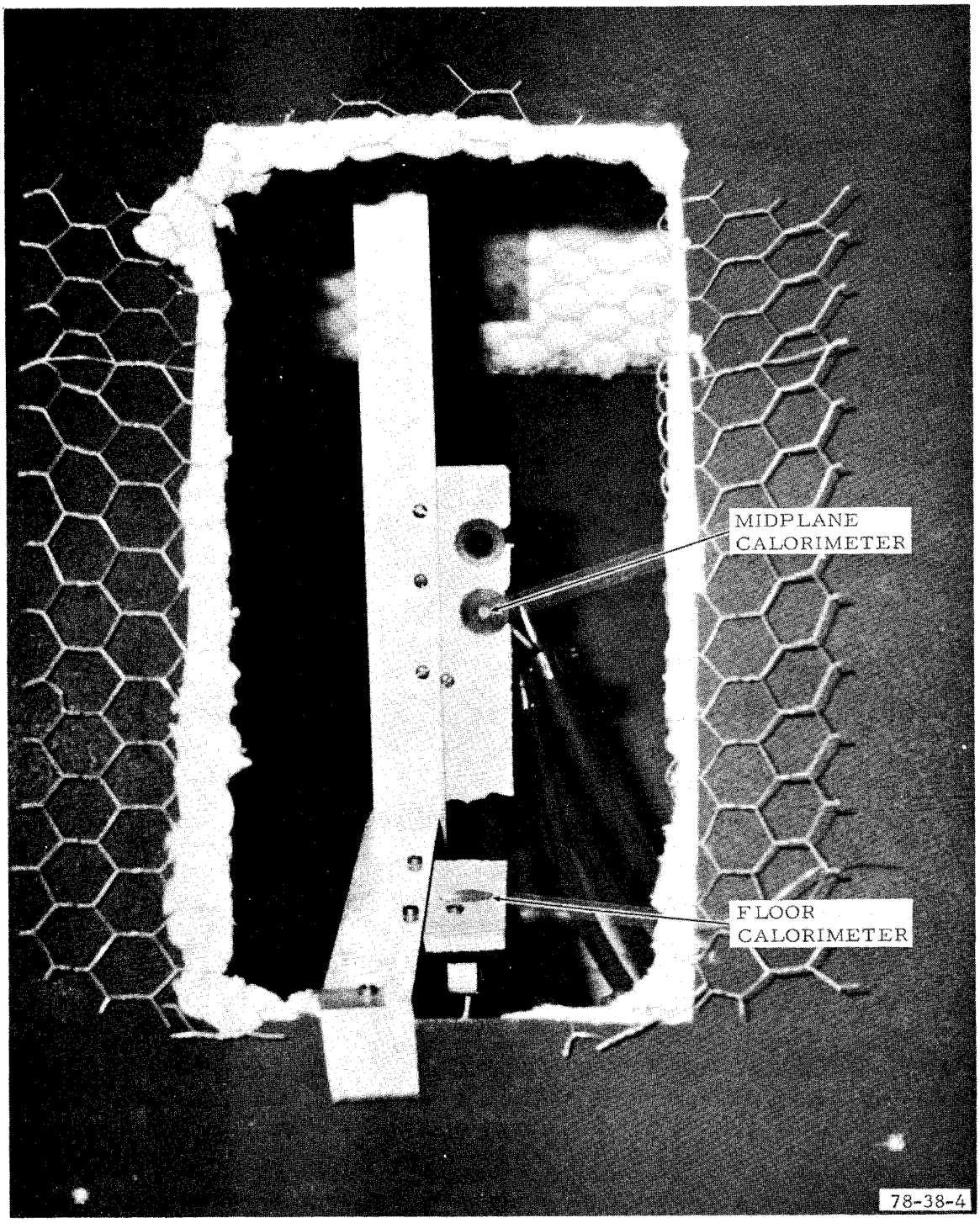

FIGURE 5. SENSORS IN 3-FOOT DUCT

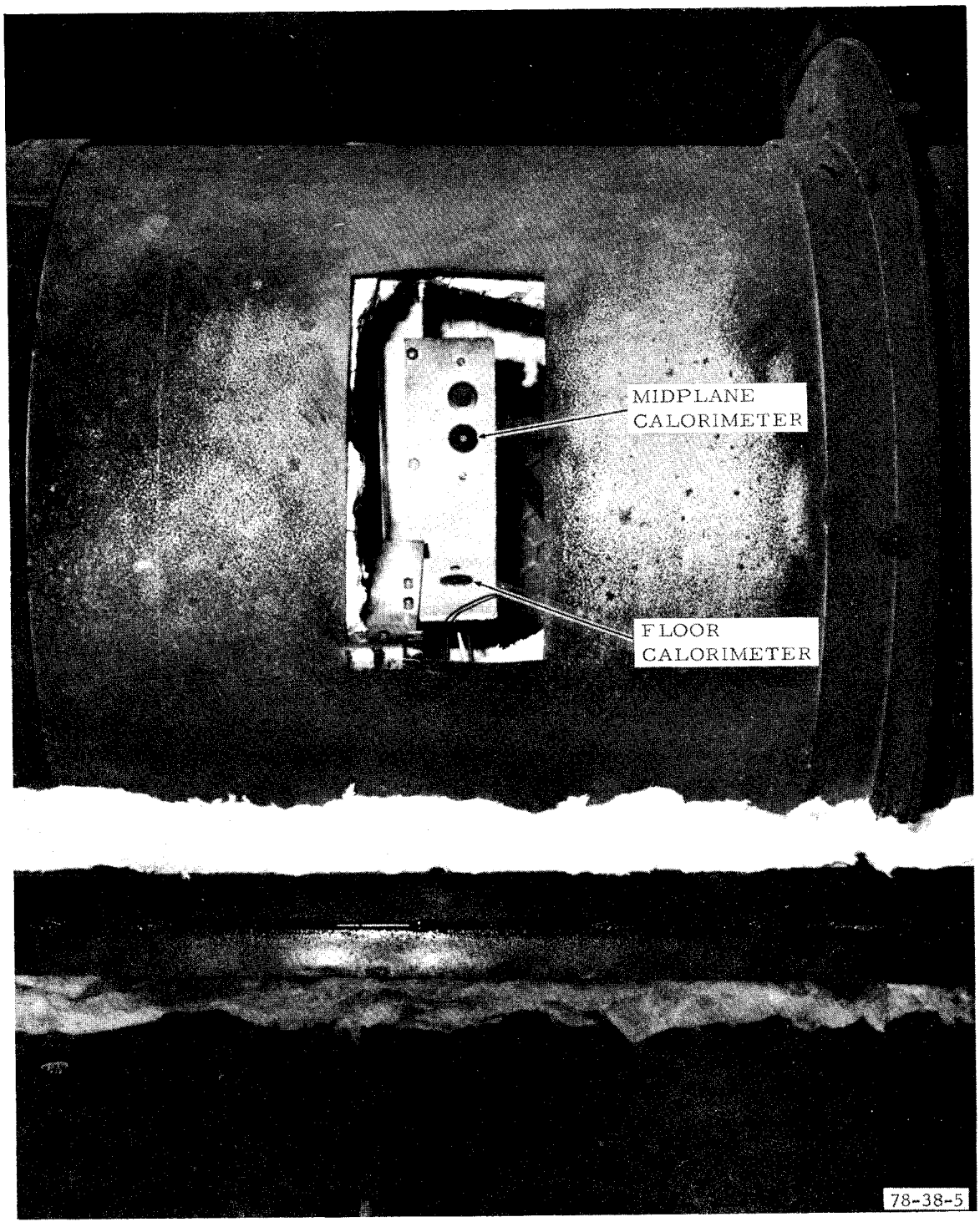

FIGURE 6. SENSORS IN 2-FOOT DUCT

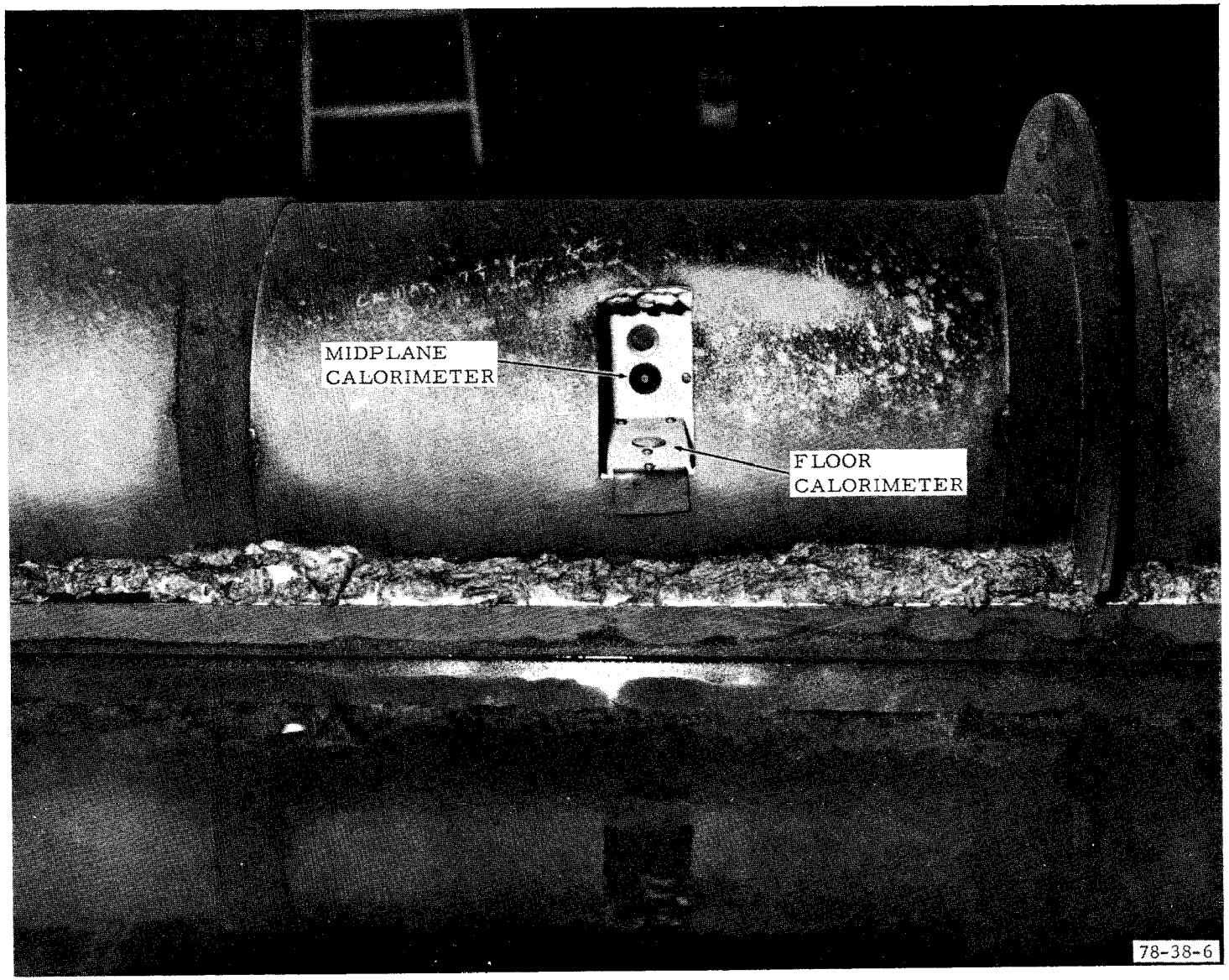

FIGURE 7. SENSORS IN 1-FOOT DUCT

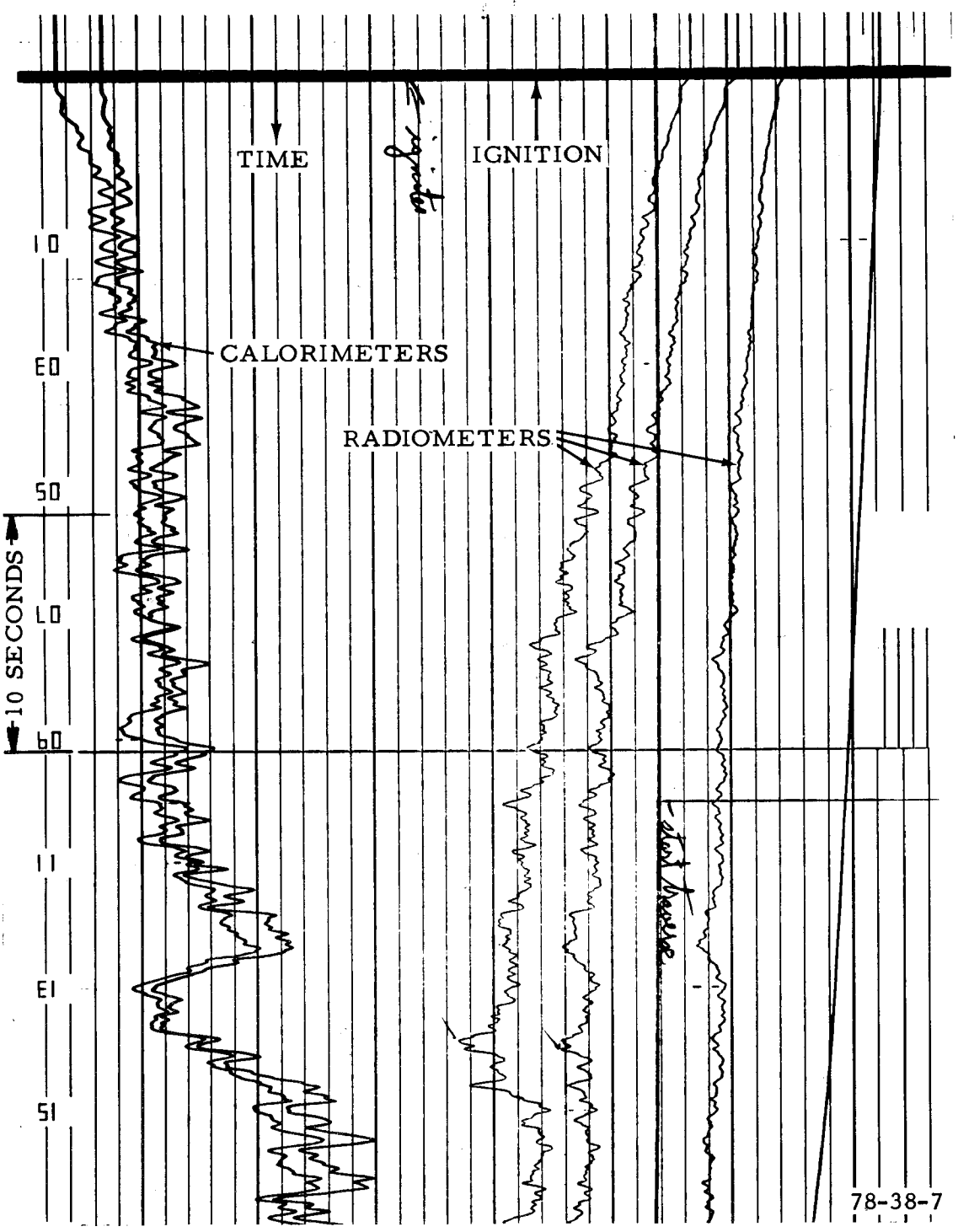

FIGURE 8. UNDAMPED OSCILLOGRAPH TRACES

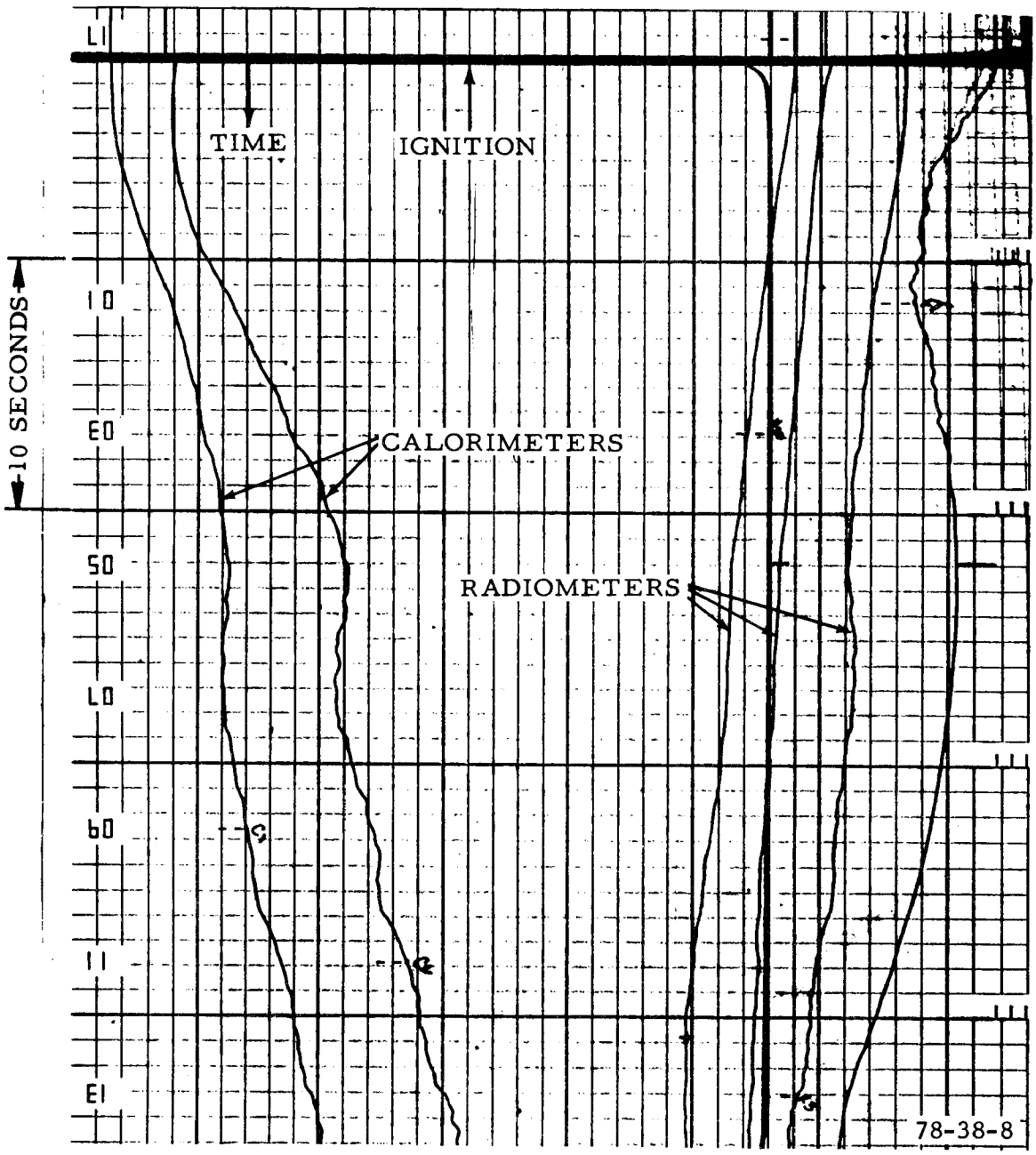

FIGURE 9. DAMPED OSCILLOGRAPH TRACES

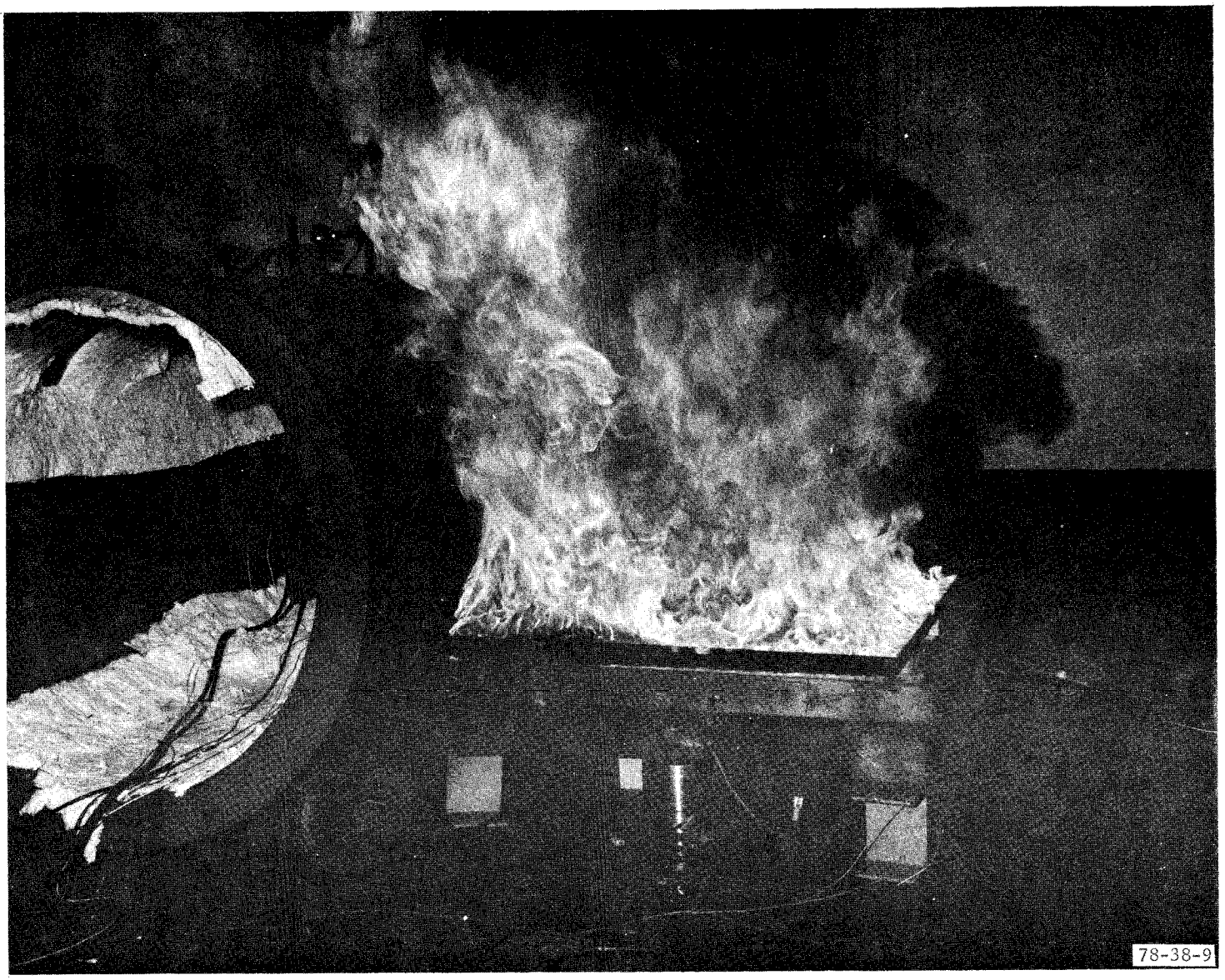

FIGURE 10. FOUR-FOOT DUCT TEST

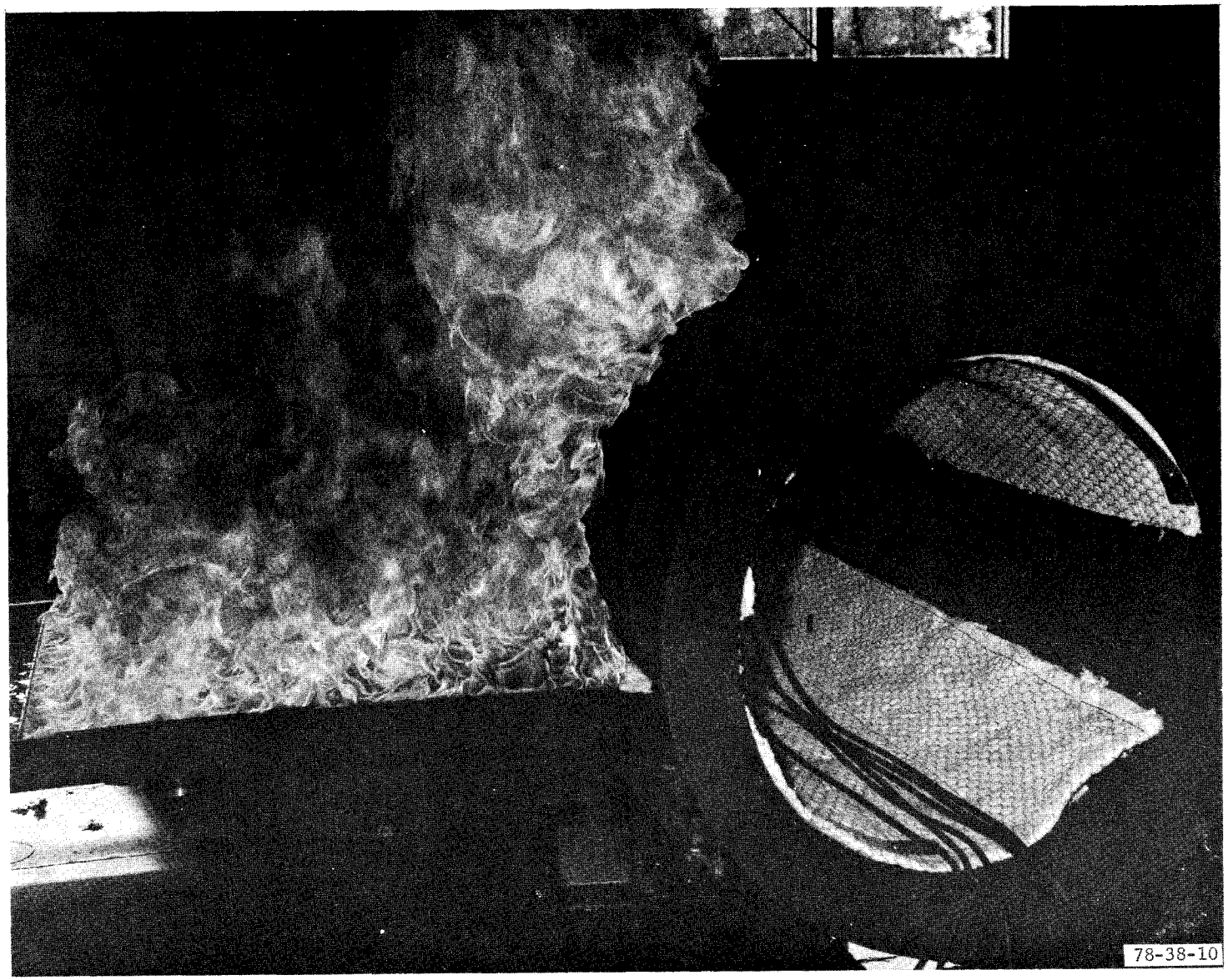

FIGURE 11. THREE-FOOT DUCT TEST

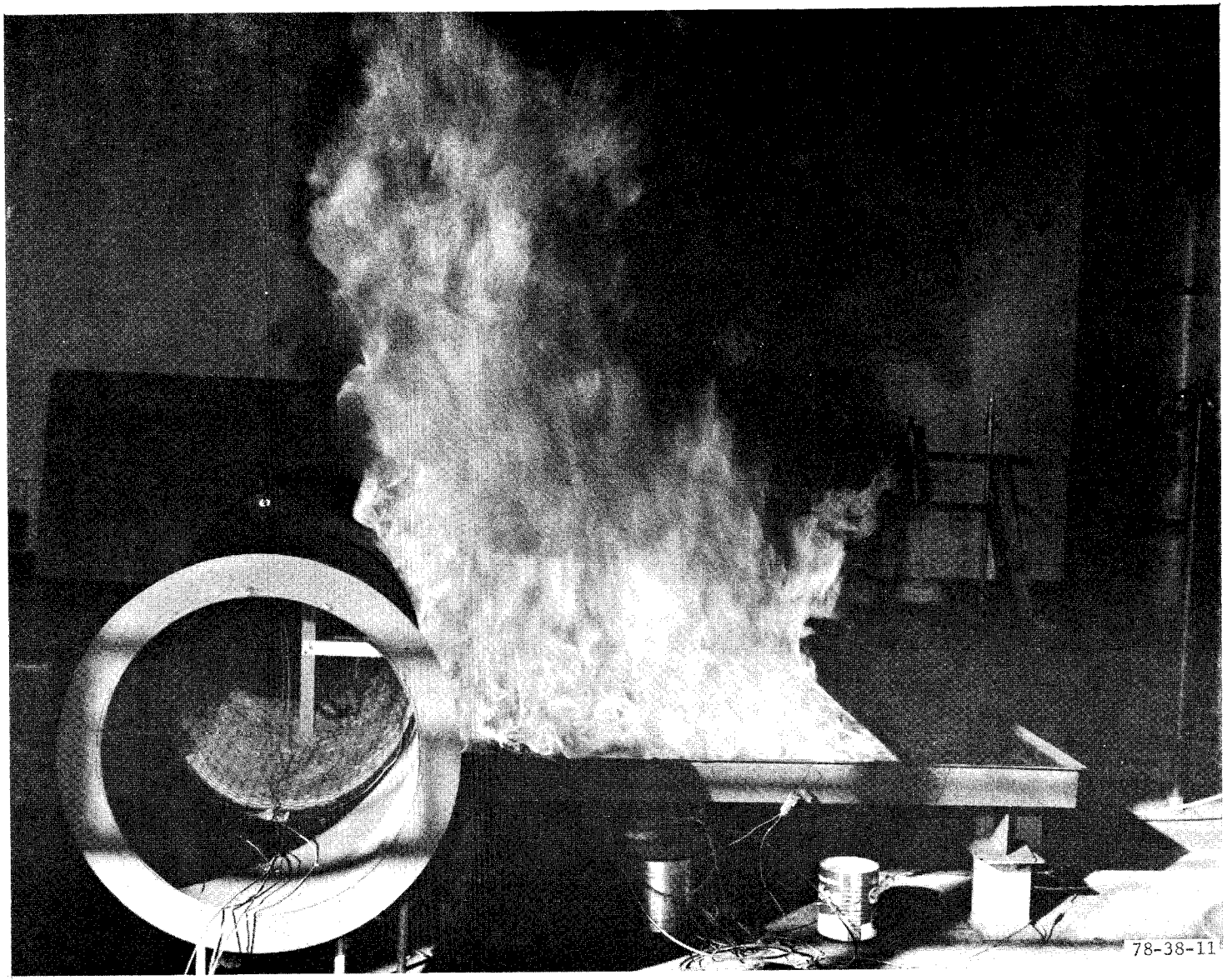

FIGURE 12. TWO-FOOT DUCT TEST

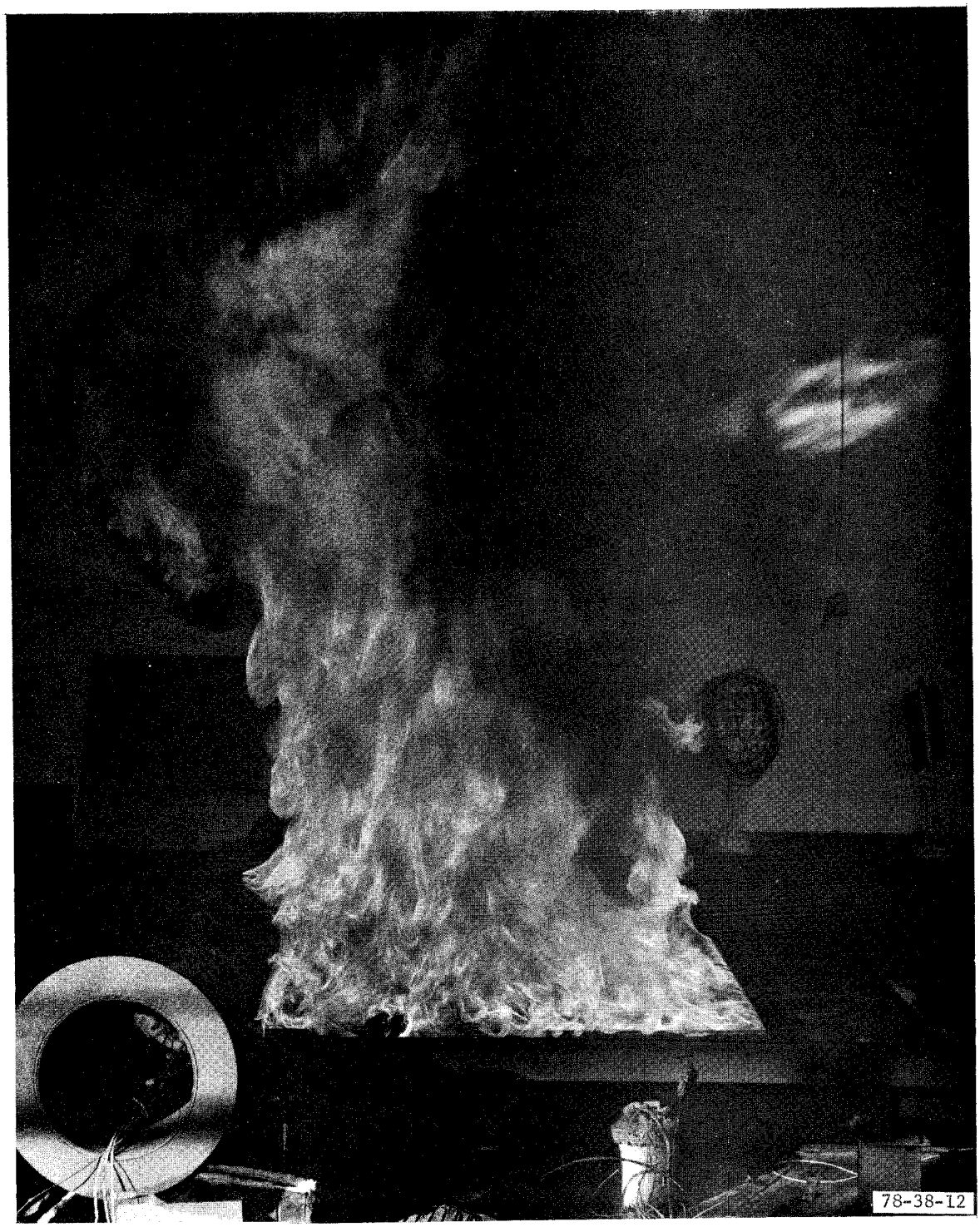

FIGURE 13. ONE-FOOT DUCT TEST

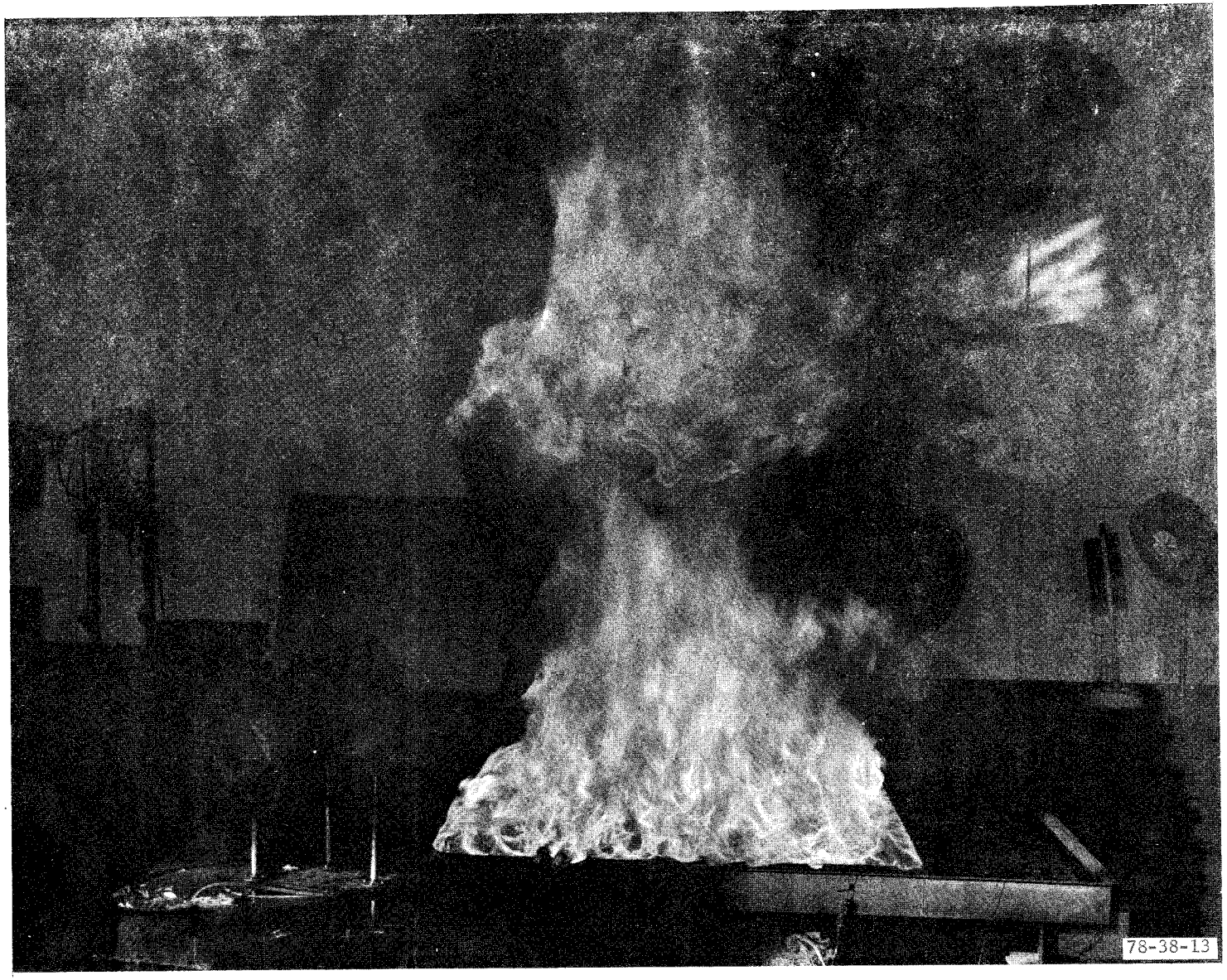

FIGURE 14. FIRE SEPARATED FROM DUCT

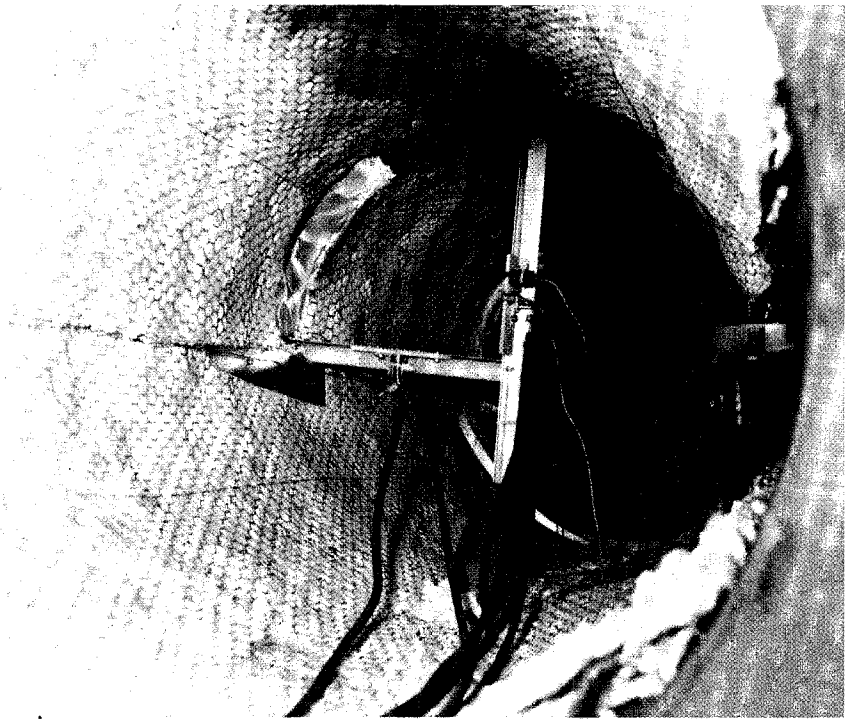

FIGURE 15a. FIRE ENGULFED DOOR RADIATING ONTO INTERIOR CALORIMETERS

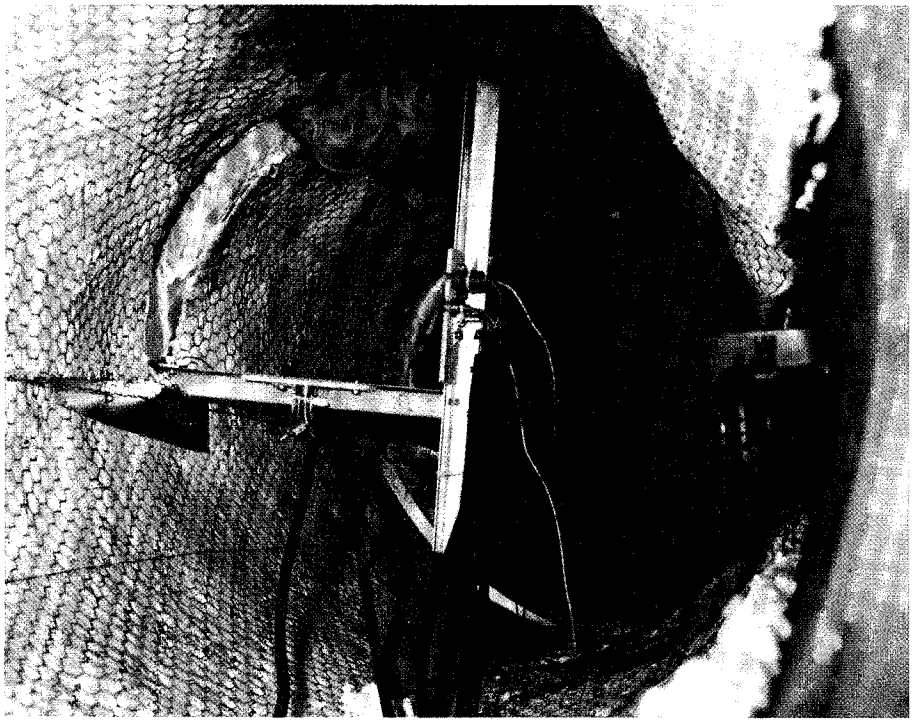

FIGURE 15b. FLAME PULSATION PENETRATING DUCT INTERIOR

FIGURE 15. INTERIOR VIEW OF FIRE

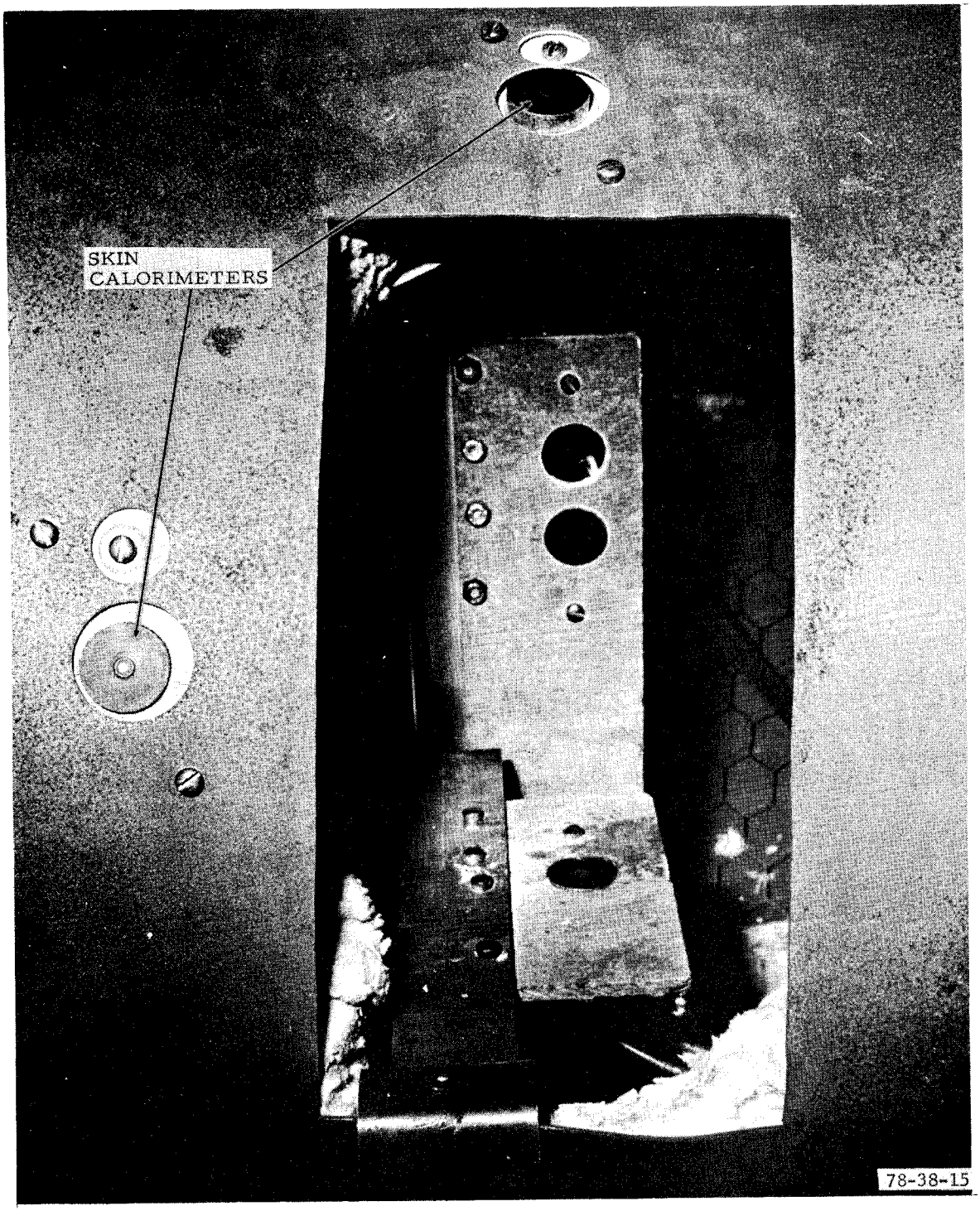

FIGURE 16. CALORIMETERS IMBEDDED IN SKIN OF 2-FOOT DUCT

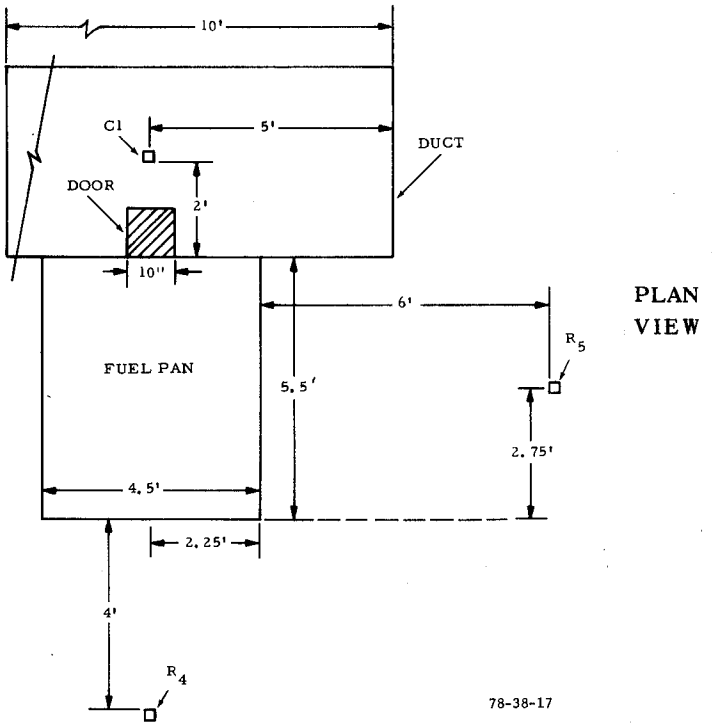

TEST NUMBER 11/29/1

Time (s)	10	20	30	40	50	60
Midplane Cal (C_1) (Btu/ft^2 s)	.5	1.1	1.4	1.3	1.5	1.5
Radiometer No. 4 (Btu/ft^2 s)	.6	1.3	1.8	1.8	1.8	1.9
Radiometer No. 5 (Btu/ft^2 s)	.4	1.0	1.3	1.4	1.5	1.7

TEST NUMBER 11/29/2

Time (s)	10	20	30	40	50	60
Midplane Cal (C_1) (Btu/ft^2 s)	.5	1.1	1.2	1.2	1.0	1.3
Radiometer No. 4 (Btu/ft^2 s)	.7	1.4	1.8	2.0	1.9	1.7
Radiometer No. 5 (Btu/ft^2 s)	.5	1.1	1.7	2.2	2.2	1.7

FIGURE 17. EXTERNAL HEAT FLUXES AND LOCATIONS

APPENDIX

RADIATION ANALYSIS

ANGLE FACTOR INTEGRAL.

Although tabulations of angle or shape factors for diffuse radiative interchange between two surfaces are readily available for simple geometries, complex geometries generally require an individual treatment. Stokes' theorem can be employed to find the angle factor in many applications (reference 15). This method involves reformulation of the angle factor surface integral equation into three separate line integrals. The coordinates are further selected so that the normal to the receiving element lies in the direction of one of the coordinates. In this way, two of the three line integrals disappear. In this type analysis the following equation must be solved:

$$F_{dA_i-A_j} = \oint_{C_j} \frac{(y_j-y_i)\,dx_j - (x_j-x_i)\,dy_j}{2\pi r^2} \qquad (1)$$

where dA_i is the receiving element, A_j is the radiating surface, and C_j is the contour around the radiating surface. In equation (1), F is the angle factor, r is the distance between a point on dA_i and another on A_j, x_i, and y_i are the positions of a point on the receiving element, and x_j and y_j are a point on the radiating surface. In this treatment, we assume the fuselage door is the radiating surface and the calorimeter is an infinitesimal receiving element. In this manner, x_i and y_i reduce to constant values.

Figure A-1 shows the parameters used to find the angle factor for the midplane calorimeter. When the center of the fuselage is taken as the origin, equation (1) can be written as follows:

$$F_{dA_i-A_j} = \oint_{C_j} \frac{(y_j-a_3)\,dx_j - x_j\,dy_j}{2\pi\left[x_j^2 + (y_j-a_3)^2 + z_j^2\right]} \qquad (2)$$

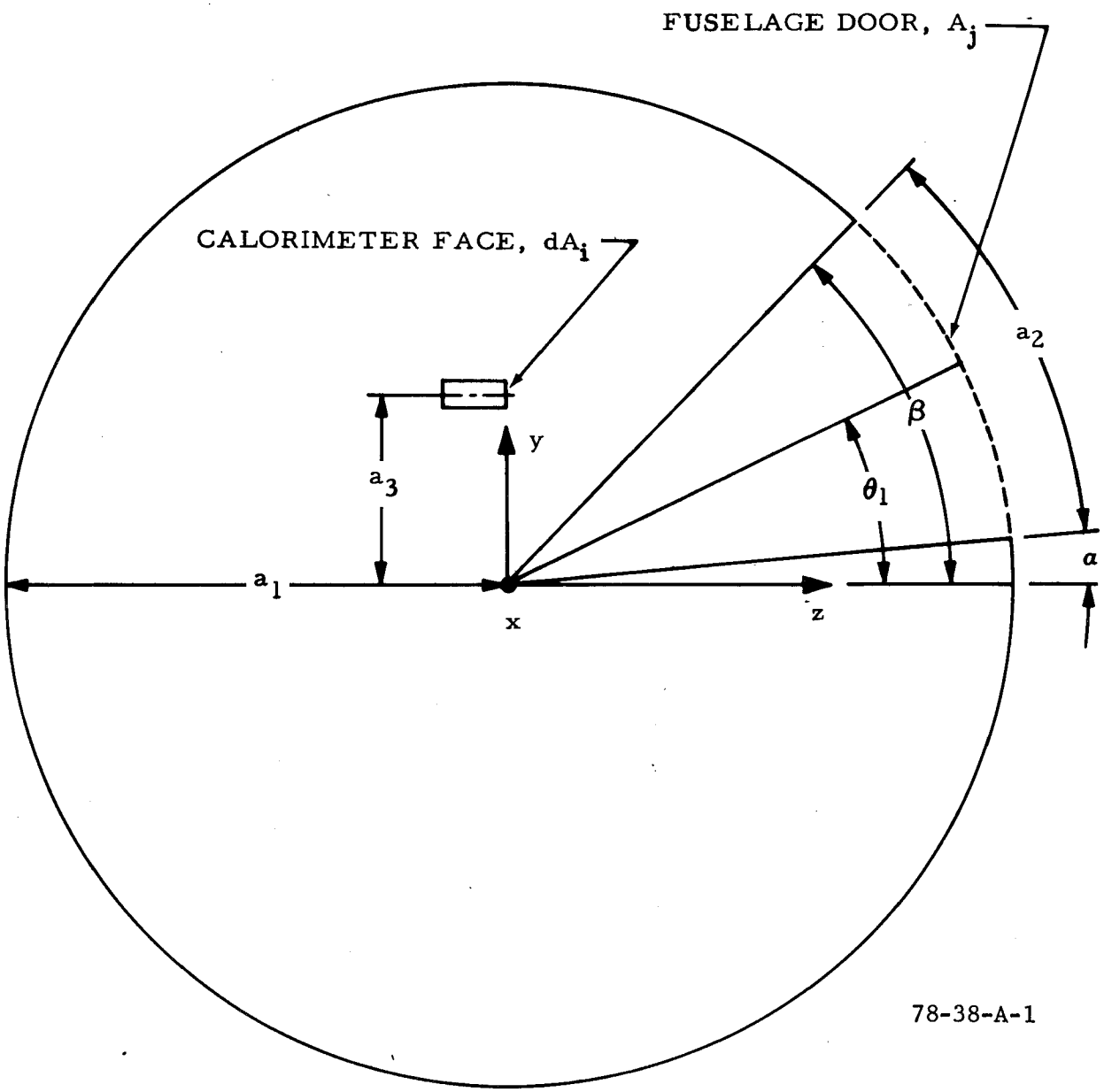

FIGURE A-1. MIDPLANE CALORIMETER COORDINATES

where: $y_j = a_1 \sin \theta_1$

$z_j = a_1 \cos \theta_1$

$dy_j = a_1 \cos \theta_1 \, d\theta_1$

$-dz_j = a_1 \sin \theta_1 \, d\theta_1$

Furthermore, the contour C_j around the door can be separated into four parts,

$$F_{dA_i - A_j} = F_1 + F_2 + F_3 + F_4 \tag{3}$$

where F_4 and F_2 are the bottom and top edge of the door, respectively, and F_1 and F_3 are the right and left door edge, respectively. Thus, looking out the door from the inside, the integrating path is counterclockwise.

If the door is of width w, the first integral is defined as follows:

$$F_1 = \int_{\alpha}^{\beta} \frac{\frac{w}{2} a_1 \cos \theta_1 \, d\theta_1}{2\pi \left[\frac{w^2}{4} + (a_1 \sin \theta_1 - a_3)^2 + a_1^2 \cos^2 \theta_1\right]} \tag{4}$$

The term $(y_j - a_3)\, dx_j$ drops out since x_j is the constant $-\frac{w}{2}$ on this length.

This integrates to make:

$$F_1 = \frac{-w}{8\pi a_3} \ln \left[1 - \frac{2a_3 a_1}{\frac{w^2}{4} + a_1^2 + a_3^2} \sin \theta_1 \right]_{\alpha}^{\beta} \tag{5}$$

where α is the angle between the z-axis and the line between the origin and door bottom. The angle between the z-axis and the line from the origin to the door top is β. The integral F_3 is identical to F_1 except that x_j is now $\frac{w}{2}$ and the order of integration limits is reversed. Thus:

$$F_1 = F_3 \tag{6}$$

The integral along the door top is written as:

$$F_2 = \int_{\frac{-w}{2}}^{\frac{w}{2}} \frac{(a_1 \sin \beta - a_3)\, dx_j}{2\pi \left[x_j^2 + (a_1 \sin \beta - a_3)^2 + a_1^2 \cos^2 \beta \right]} \qquad (7)$$

and this integrates out as:

(8)

$$F_2 = \frac{a_1 \sin \beta - a_3}{2\pi} \frac{1}{\sqrt{a_1^2 + a_3^2 - 2a_1 a_3 \sin \beta}} \tan^{-1} \left\{ \frac{x_j}{\sqrt{a_1^2 + a_3^2 - 2a_1 a_3 \sin \beta}} \right\} \Bigg]_{\frac{-w}{2}}^{\frac{w}{2}}$$

The integral along the bottom of the door is written:

$$F_4 = \int_{\frac{w}{2}}^{\frac{-w}{2}} \frac{-a_3\, dx_j}{2\pi \left[x_j^2 + (a_1 \sin \alpha - a_3)^2 + a_1^2 \cos^2 \alpha \right]} \qquad (9)$$

Both equation (7) and (9) are integrated along a line where the y variable is held constant and thus the numerator under the integral reduces to one term. Equation (9) integrates to form:

$$F_4 = \frac{-a_3}{2\pi} \frac{1}{\sqrt{a_1 2 + a_3 2 - 2a_1 a_3 \sin\alpha}} \tan^{-1} \frac{x_j}{\sqrt{a_1^2 + a_3^2 - 2a_1 a_3 \sin\alpha}} \Bigg]_{\frac{w}{2}}^{\frac{-w}{2}} \quad (10)$$

Figure A-2 shows the variables for evaluating the angle factor for a calorimeter on the floor. As in the midplane calorimeter solution, equation (1) is applied to the geometrical arrangement shown in figure A-2. In this case,

$$F_{dA_i - A_j} = \oint_{C_j} \frac{(y_j - a_4)dx_j - x_j\, dy_j}{2\pi \left[x_j^2 + (y_j - a_4)^2 + z_j^2\right]} \quad (11)$$

where: $x = x_j$

$y_j = a_1 \cos\theta_1$

$z_j = a_1 \sin\theta_1$

$dy_j = -a_1 \sin\theta_1\, d\theta_1$

$dz_j = a_1 \cos\theta_1\, d\theta_1$

Once again the integral is broken into four parts, as shown in equation (4), with the same direction of integration and the same identification of the door sides. Along the right side of the door, x_j is simply half the door width or $\frac{w}{2}$, and

$$F_1 = \int_{\alpha}^{\beta} \frac{\frac{w}{2} a_1 \sin\theta_1\, d\theta_1}{2\pi \left[\frac{w^2}{4} + (a_1 \cos\theta_1 - a_4)^2 + a_1{}^2 \sin^2\theta_1\right]} \quad (12)$$

which integrates out to form:

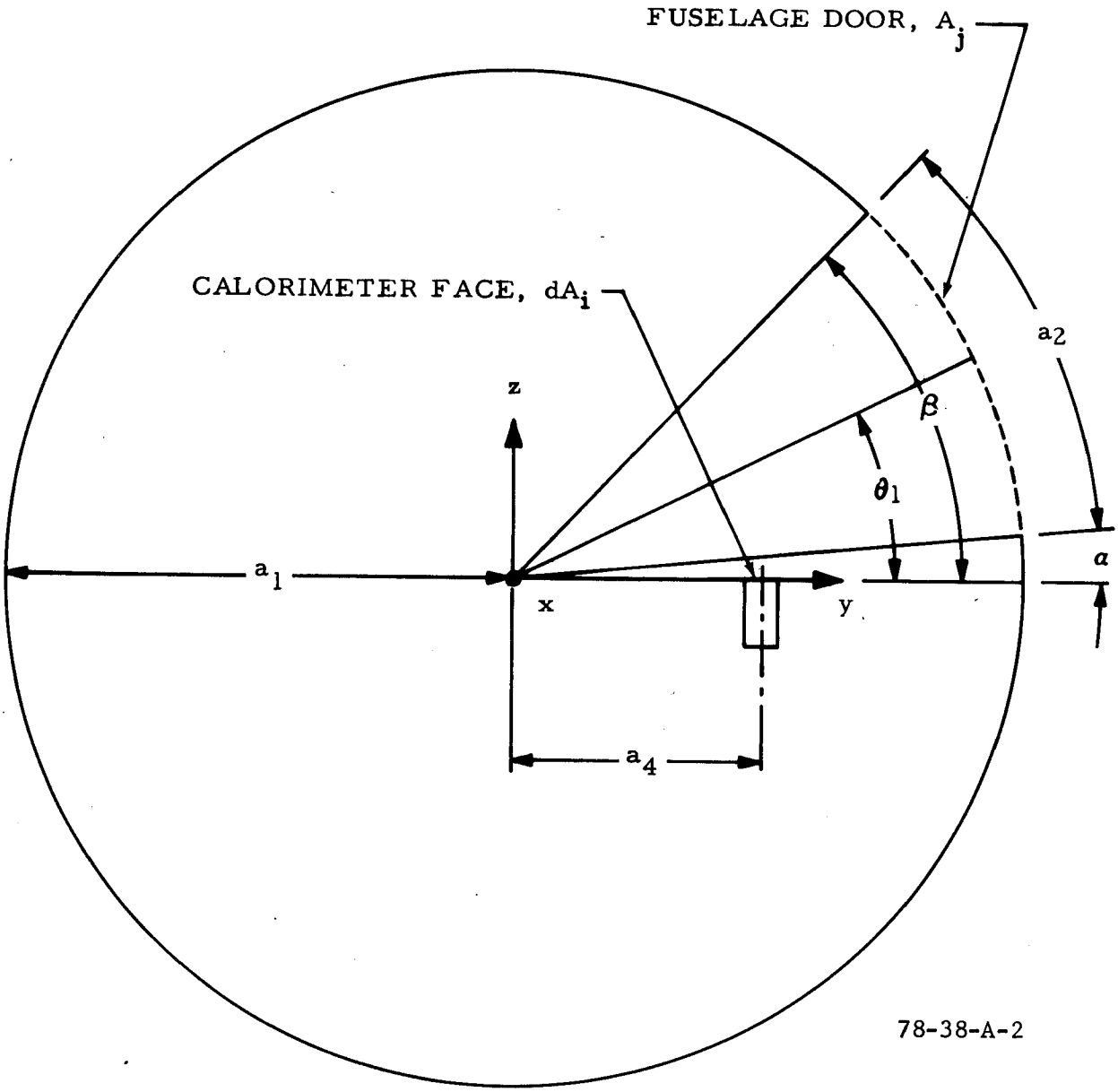

FIGURE A-2. FLOOR CALORIMETER COORDINATES

$$F_1 = \frac{w}{8\pi a_4} \ln \left[1 - \frac{2a_1 a_4}{\frac{w^2}{4} + a_1^2 + a_4^2} \cos\Theta_1 \right]_{\alpha}^{\beta} \qquad (13)$$

By reasoning identical to that used in the midplane calorimeter solution, F_1 equals F_3, and two of the four needed integrations are complete. Along the top of the door, y and z are constant and the integral is stated as:

$$F_2 = \int_{\frac{w}{2}}^{\frac{-w}{2}} \frac{\left[a_1 \cos\beta - a_4 \right] dx_j}{2\pi \left[x_j^2 + (a_1 \cos\beta - a_4)^2 + a_1^2 \sin^2\beta \right]} \qquad (14)$$

and this is solved as:

(15)

$$F_2 = \frac{(a_1 \cos\beta - a_4)}{2\pi\sqrt{(a_1 \cos\beta - a_4)^2 + a_1^2 \sin^2\beta}} \tan^{-1}\left[\frac{x_i}{\sqrt{a_1^2 + a_4^2 - 2a_1 a_4 \cos\beta}} \right]_{\frac{w}{2}}^{\frac{-w}{2}}$$

The integral along the door bottom is stated as:

$$F_4 = \int_{\frac{-w}{2}}^{\frac{w}{2}} \frac{\left[a_1 \cos\alpha - a_4 \right] dx_j}{2\pi \left[x_j^2 + (a_1 \cos\alpha - a_4)^2 + a_1^2 \sin^2\alpha \right]} \qquad (16)$$

and solved as:

(17)

$$F_4 = \frac{a_1 \cos\alpha - a_4}{2\pi\sqrt{a_1^2 - 2a_1a_4\cos\alpha + a_4^2}} \tan^{-1} \frac{x_j}{\sqrt{a_1^2 - 2a_1a_4\cos\alpha + a_4^2}} \Bigg]_{-\frac{w}{2}}^{\frac{w}{2}}$$

CALCULATIONS.

Because all four ducts used in the tests have the same ratio of door width and length to fuselage diameter, any angle factor solution for one sized duct is the solution for all four ducts as long as the relative placement of the calorimeter is the same.

The following dimensions will be used for a solution:

$\frac{w}{2}$ = 2.56 inches

a_2 = 10.75 inches

a_1 = 12 inches

a_3 = 3 inches

a_4 = 6 inches

α = 0°

β = 51.33°

Using these numbers, the angle factor for the midplane calorimeter, F_M is 0.127 and the angle factor for the floor calorimeter F_F is 0.172. The ratio F_F/F_M is 1.35 and this agrees well with the measurements for the 1-, 2-, and 3-foot diameter ducts adjacent to a 4-foot square fuel pan.

RADIATIVE FLUX.

The radiative flux between two surfaces is given as:

$$q = \varepsilon \sigma T^4 F_{dA_i - A_j} \qquad (18)$$

where q is the heat flux, ε the surface emissivity, T the absolute temperature, and σ the Stefan-Boltzmann constant. Using 0.127 as the angle factor for the midplane calorimeter and 1.8 Btu/ft^2 s as experimental heat flux, equation (18) can be solved to yield a blackbody temperature of 1874°F when the emissivity is taken as unity.

When this temperature is used along with the relations developed for angle factors, heat fluxes in the vicinity of the door can be readily calculated on a point-by-point basis. Using the procedures developed here, a number of heat flux profiles were calculated for the cabin interior. Figure A-3 shows the calculated heat flux incident at the cabin midplane at a height of 3 inches above the floor as the receiving element is moved parallel to the fuselage centerline. Figure A-4 shows the heat flux incident at the cabin midplane as the receiving element is moved vertically. What is apparent from these calculations is the flatness of the heat flux profile within the door outline. Objects perpendicular to the door will all be subject to similar values of heat flux. This observation was experimentally confirmed by the traversing calorimeter which encountered little change in heat flux as it moved from one end of the door to the other along the fuselage midplane.

Figure A-5 shows the heat flux as the receiving element is moved along the floor from the middle of the duct door directly back to the fuselage midplane. In this plot, the range of incident heat fluxes is significant. Flooring materials close to the doorway are subject to much higher radiant heat fluxes than materials on the floor in the middle of the fuselage. Figure A-6 shows the heat flux to the receiver on the floor at a distance of 3 inches back from the door as the receiver moves parallel to the fuselage centerline. The change in absolute value of heat flux is minimal around the door itself. The flux does significantly drop as the receiver is moved to an interior position approximately one door width beyond the door edge.

In figures A-3 through A-6, the calculated shape factor between the receiver and the door is simultaneously plotted. The shape factor and the incident heat flux differ by a constant factor when a uniform blackbody temperature across the door opening is assumed. In addition, the positions in the figures are given in generalized notation related to the fuselage diameter and door width. Since all four duct sizes used in the tests were geometrically similar, the radiation calculations are applicable to all cases when the dimensions are generalized.

$$q = \varepsilon \sigma T^4 F_{dA_i - A_j} \qquad (18)$$

where q is the heat flux, ε the surface emissivity, T the absolute temperature, and σ the Stefan-Boltzmann constant. Using 0.127 as the angle factor for the midplane calorimeter and 1.8 Btu/ft^2 s as experimental heat flux, equation (18) can be solved to yield a blackbody temperature of 1874°F when the emissivity is taken as unity.

When this temperature is used along with the relations developed for angle factors, heat fluxes in the vicinity of the door can be readily calculated on a point-by-point basis. Using the procedures developed here, a number of heat flux profiles were calculated for the cabin interior. Figure A-3 shows the calculated heat flux incident at the cabin midplane at a height of 3 inches above the floor as the receiving element is moved parallel to the fuselage centerline. Figure A-4 shows the heat flux incident at the cabin midplane as the receiving element is moved vertically. What is apparent from these calculations is the flatness of the heat flux profile within the door outline. Objects perpendicular to the door will all be subject to similar values of heat flux. This observation was experimentally confirmed by the traversing calorimeter which encountered little change in heat flux as it moved from one end of the door to the other along the fuselage midplane.

Figure A-5 shows the heat flux as the receiving element is moved along the floor from the middle of the duct door directly back to the fuselage midplane. In this plot, the range of incident heat fluxes is significant. Flooring materials close to the doorway are subject to much higher radiant heat fluxes than materials on the floor in the middle of the fuselage. Figure A-6 shows the heat flux to the receiver on the floor at a distance of 3 inches back from the door as the receiver moves parallel to the fuselage centerline. The change in absolute value of heat flux is minimal around the door itself. The flux does significantly drop as the receiver is moved to an interior position approximately one door width beyond the door edge.

In figures A-3 through A-6, the calculated shape factor between the receiver and the door is simultaneously plotted. The shape factor and the incident heat flux differ by a constant factor when a uniform blackbody temperature across the door opening is assumed. In addition, the positions in the figures are given in generalized notation related to the fuselage diameter and door width. Since all four duct sizes used in the tests were geometrically similar, the radiation calculations are applicable to all cases when the dimensions are generalized.

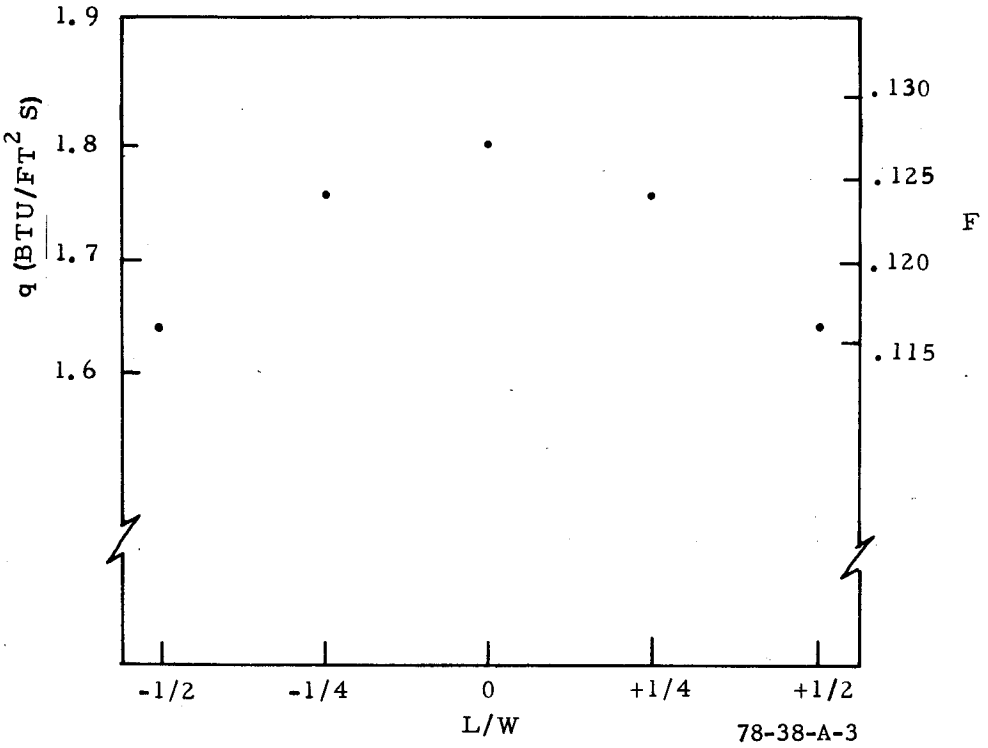

FIGURE A-3. VARIATION OF MIDPLANE RADIATION AS RECEIVING ELEMENT IS DISPLACED FROM CENTER OF DOORWAY (L IS HORIZONTAL DISTANCE FROM DOOR CENTER, a_3/w is 0.59)

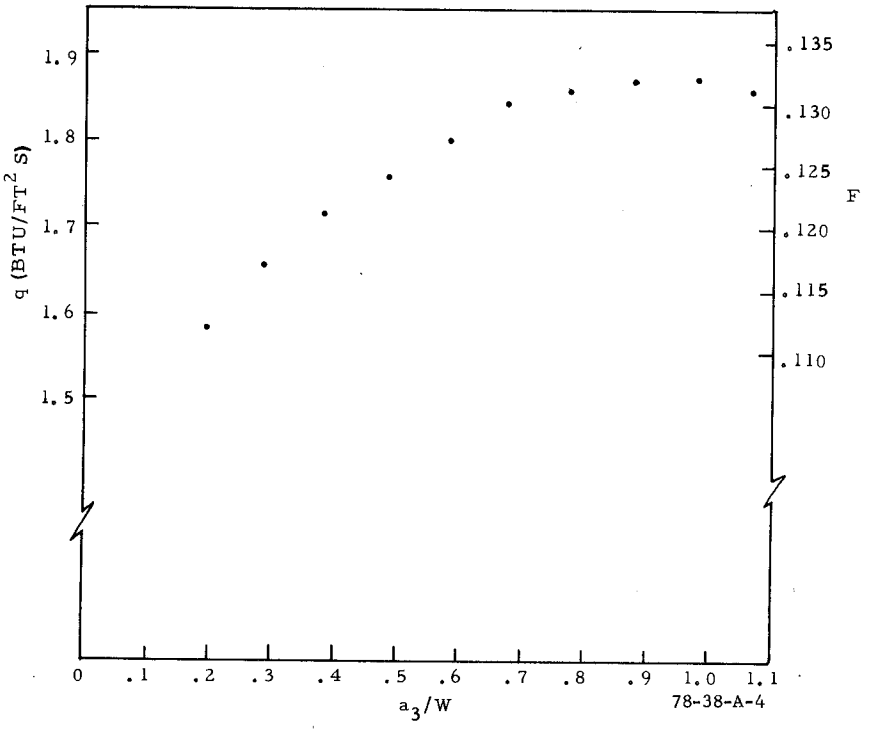

FIGURE A-4. VARIATION OF MIDPLANE RADIATION WITH HEIGHT

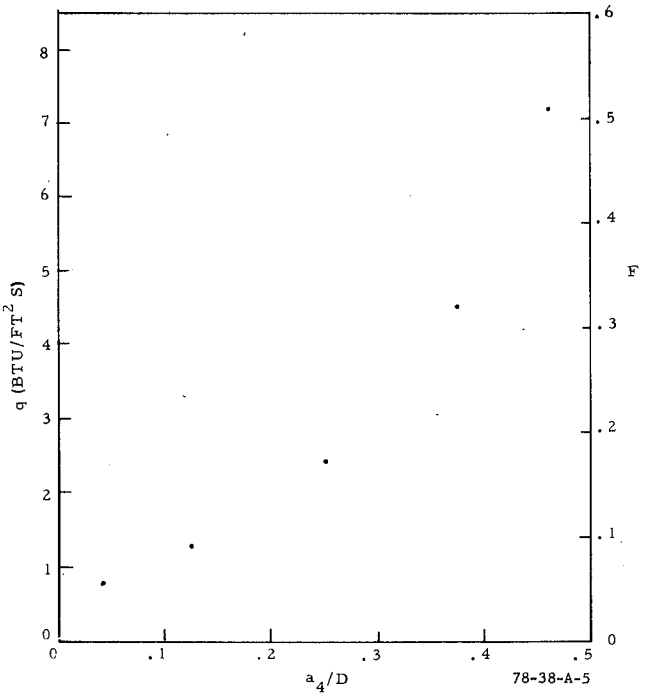

FIGURE A-5. VARIATION OF FLOOR HEAT FLUX BETWEEN DOOR EDGE AND DUCT MIDPLANE (D IS FUSELAGE DIAMETER)

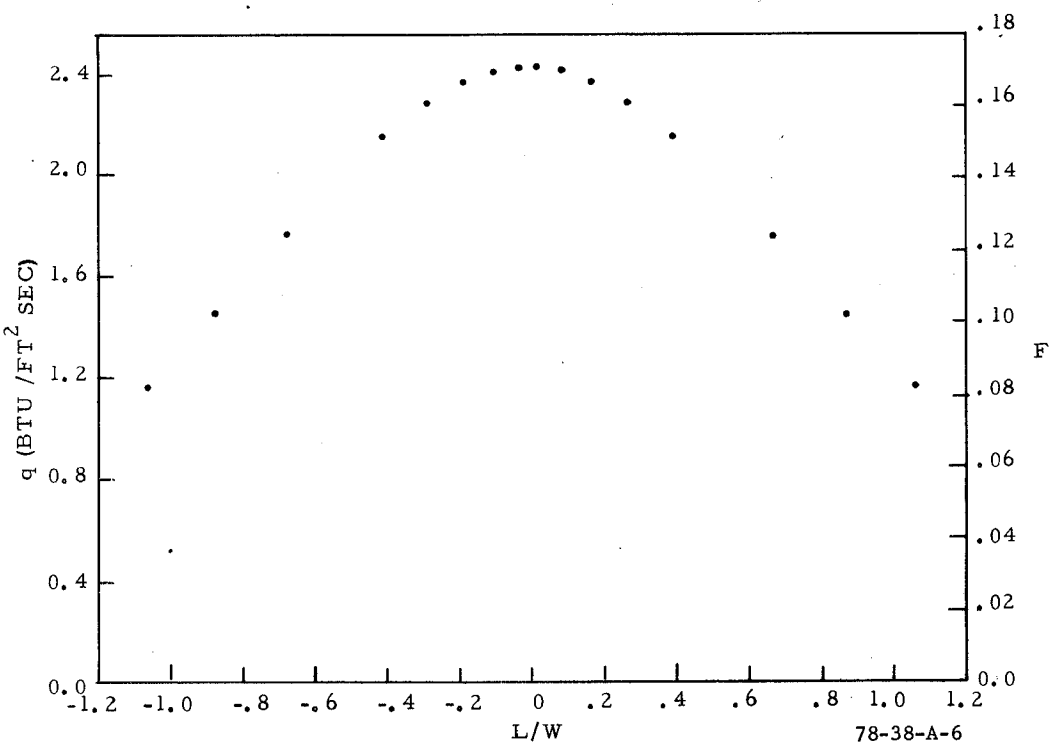

FIGURE A-6. VARIATION OF FLOOR HEAT FLUX AS RECEIVING ELEMENT IS DISPLACED FROM CENTER OF DOORWAY (L IS HORIZONTAL DISTANCE FROM DOOR CENTER, a_4/D is 0.250)